Chapter 2

A Review of the Literature on Column Flotation Modeling

2.1 Introduction

The increasing acceptance of column flotation technology in the mineral processing industry has encouraged a significant amount of research. This research is mainly aimed at the prediction of column performance through mathematical representations of the various subprocesses taking place in a flotation column. A number of approaches have been followed, based mainly on the amount of detail sought and the intended application.

Studies of two-phase (air-water) system behavior, for instance, have helped provide better insight into the flow conditions and characteristics of froth. However, the development of three-phase models capable of predicting metallurgical performance is still the primary motive for column modeling. Some modeling efforts have looked into the relationships between column geometry and performance. These models generally constitute an aide in column scale-up and design. The majority of researchers, however, have followed the methodology commonly used by chemical engineers of incorporating both the physical and chemical conditions into a kinetic rate constant directly related to recovery. Quantitative knowledge of all the subprocesses is not necessary in this case. However, when the objective is to understand the interrelationships between several particulate phases throughout the column, the number of parameters involved has made such models impracticable for industrial applications.

Kinetic models, as well as the supporting equations relating the model parameters to operating conditions, have become the foundation for most steady-state simulators. On the other hand, the introduction of model-based control techniques into the field of mineral processing has resulted in a need for the development of dynamic models. In this regard, the use of phenomenological models, such as population balance models, is the course proposed by many investigators. The phenomena that cannot yet be described through mathematically tractable equations are represented with a set of lumped parameters whose values are determined from experimental data. In other instances, empirical models derived from experimental dynamic response data are utilized to investigate the performance of computer control techniques.

With the increase in the number of publications on column flotation in the last decade, several reviews on this general subject are available (Tuteja et al., 1994; Finch and Dobby, 1991). The aim of this chapter is to provide an inclusive survey of the progress made in the specific area of column flotation modeling. Such examination also presents an overview of the different modeling approaches taken and an indication of the challenges that remain. A broad list of the flotation subprocesses reviewed includes bubble-particle

(collision, attachment and detachment) and bubble-bubble (coalescence) interactions, hydrodynamic conditions in the pulp (mixing, flow regime), and froth behavior (stability, drainage).

In addition, the endeavor to understand and predict column flotation behavior is supported to a considerable extent by earlier work on conventional froth flotation. Other related fields include: studies of gas-liquid and gas-liquid-solid systems in chemical engineering (especially drift-flux analysis), theory of packed and fluidized beds, studies of flow regimes in bubble reactors, dispersion modeling, and reaction kinetics. For this reason, several papers on general flotation modeling, as well as literature on other processes from which model developers have derived fundamental relationships, are included in this review.

2.2 Background

Flotation columns first appeared on the market in the late 1960's as an innovation in the field of froth flotation. Columns offered a solution, or at least an improvement, with respect to some of the problems encountered with conventional flotation cells. The most evident was the higher length-to-diameter ratio, which can be visualized as a series of vertically stacked cells. This geometry, along with the elimination of impellers inside the unit, favored a more quiescent environment. Such an environment was thought to be beneficial to recovery, while eliminating the need for long banks of conventional cells. The other important difference from conventional flotation was the creation of a deep froth with water added at the top. The goal of such modification was to wash down particles entrained in the spaces between bubbles and eliminate or minimize non-selective entrainment of gangue.

Despite their potential, it has only been in the last ten to fifteen years that flotation columns have become popular in the mineral processing industry. This rise in popularity can be partially attributed to progress made in the development of scale-up, design and operational procedures. Such knowledge has developed from both the theoretical analysis of the phenomena, and the practical experience gained by studying the impact of different column geometries and operating settings on column performance. By translating this information into a mathematical model, it can be applied in predicting the necessary size, flowrates, zone levels and other parameters that are required to meet a defined objective.

In this review, mathematical representations of flotation columns are classified into two categories. The first consists of two-phase models developed from a consideration of the column as a gas-liquid system. The second comprises three-phase models developed from a consideration of the column as a gas-liquid-solid system. Within each of these categories, modeling of the pulp and froth zones has often been tackled independently.

2.3 Two-Phase Models

2.3.1 Column Hydrodynamics

Hydrodynamic models are used to describe the flow conditions that are prevalent in a reactor. In column modeling, they relate parameters such as bubble size, air fraction, gas and liquid velocities, and bubble and liquid densities. Their significance lies mainly in the fact that column hydrodynamics affects the chances of bubble-particle contact, the residence time of the various phases, and the extent of mixing inside the column cell. The solids residence time and the degree of axial dispersion, in turn, are directly linked to the recovery of minerals. Studies of the hydrodynamic conditions in an air-water system provide the background upon which a representation of the gas-slurry can be built.

Study of the column hydrodynamic conditions is based on the theory of dispersed multiphase flows. The modeling technique employed is known as the drift-flux model, which results from a momentum conservation equation for the multiphase mixture. Drift-flux modeling is based on the relative velocity between the phases. Such relative velocity is given by algebraic relationships.

In column flotation, drift flux theory states that the hindered bubble rise velocity (Ugs), is defined by:

$$Ugs = \frac{Jg}{\varepsilon_g} - \frac{Jl}{1-\varepsilon_g} \qquad [1]$$

where Jg is the superficial gas velocity, Jl is the superficial liquid velocity, and ε_g is the fractional air holdup. Equation [1], along with the following general hindered settling equation for Non-Stokes flow (Masliyah, 1979)

$$Ugs = Vi - Vf = \frac{gDi^2 F(\varepsilon_f)(\rho_i - \rho_{susp})}{18\mu_f (1 + 0.15 Re_s^{0.687})}, \qquad [2]$$

has been used to estimate average bubble size in the collection zone (Yianatos et al., 1988), where g refers to the gravitational acceleration, Di is the diameter of the i-th bubble size class, ε_f is the liquid volumetric fraction, ρ_i is the density of bubbles in the i-th size class, ρ_{susp} is the suspension density; and μ_f is the liquid viscosity. An iterative technique has been used in conjunction with the following expression for the bubble Reynolds number (Re_s):

$$Re_s = \frac{Di(Vi - Vf)\rho_f \varepsilon_f}{\mu_f} \qquad [3]$$

to solve these equations. The terms *Vi* and *Vf* indicate the average bubble and liquid velocities, respectively.

Several expressions for F(ε_f) in Equation [2] have been empirically obtained and reported (Richardson and Zaki, 1954; Marrucci, 1965; Turner, 1966; Davidson and Harrison, 1966; Bhaga and Weber, 1972; Lockett and Kirkpatrick, 1975). One of the most widely used is the Richardson-Zaki relationship, where

$$F(\varepsilon_f) = \varepsilon_f^{\,m-2} \qquad [4]$$

and *m* is defined as follows:

for *Re* < 200, $m = 4.45 + 18\left(\frac{Db}{Dc}\right)Re^{-0.1}$ [5]

for 200 < *Re* < 500, $m = 4.45Re^{-0.1}$ [6]

for *Re* > 500, $m = 2.39$ [7]

Here $Re = \frac{Db.Ut.\rho_f}{\mu_f}$ [8]

is the Reynolds number for a single bubble rising in a liquid, *Db* is the bubble diameter, *Dc* is the column cross sectional area, and

$$Ut = \frac{Ugs}{\varepsilon_f^{\,m-1}} \qquad [9]$$

is the terminal rise velocity of a single bubble.

Although the Richardson-Zaki expression is considered suitable for air fractions less than 30 %, some investigators have preferred the Marrucci equation (Marrucci, 1965) because it was derived using a theoretical analysis of the fluid surrounding each bubble so it is not just an empirical correlation. This equation states that

$$\frac{U_{gs}}{U_t} = \frac{1-\varepsilon_g}{1-\varepsilon_g^{5/3}} \qquad [10]$$

and it is valid for air fractions up to 20%. Lockett and Kirkpatrick (1975) tested several equations proposed against a set of experimentally determined values of air fraction and rise velocity.

A correction factor was introduced to account for the discrepancy between the data at air holdups greater than 30% and the Richardson and Zaki correlation. This correction factor is given as:

$$\frac{U_{gs}}{U_t} = \left(1-\varepsilon_g\right)^{n-1}\left(1+2.55\varepsilon_g^{\,3}\right). \qquad [11]$$

Dobby, Yianatos and Finch (1988) also used the drift flux model to estimate average bubble size below 0.2 cm in gas-water systems and in gas-slurry systems. However, they applied the following two equations:

$$Ut = \frac{v_g}{\varepsilon_g\left(1-\varepsilon_g\right)^m} - \frac{\left(v_g + v_f\right)}{\left(1-\varepsilon_g\right)^m} \qquad [12]$$

$$\text{and } Db = \left[\frac{18\mu_f Ut}{g\Delta\rho}\left(1+0.15\,\mathrm{Re}_s^{\,0.687}\right)\right]^{1/2} \qquad [13]$$

where v_g represents the average superficial gas velocity, v_f signifies the average superficial liquid velocity, and $\Delta\rho$ represents the difference between the bubble and liquid densities. This method was also incorporated in the development of a column model by other workers (Alford, 1992).

An alternative method of estimating *Db* for values less than 2 mm is the correlation developed by Clift et al (1978), which for water at 20° C is approximated by

$$Ut = 48.9Db^{0.514} - 0.309Db^{-1} \qquad [14]$$

For bubble diameters greater than 2 mm, Yianatos et al. (1988) adopted the concept of tortuosity for estimating bubble size. This concept is based on the idea that larger bubbles oscillate causing a decrease in the rise velocity and resulting in a larger effective path. The tortuosity term was estimated previously in another work (Yianatos et al., 1985) from both geometric and statistical analyses. It was initially applied as a correction factor for holdup measurements using conductivity probes.

A non-iterative technique for estimating bubble size in a flotation column was introduced by Ityokumbul et al. (1995). This method was also based on the calculation of bubble terminal velocity from drift flux relationships. However, the authors did not employ a single drift flux expression. They correlated bubble terminal rise velocities from literature data with bubble size for different frother systems and determined the drift flux expression that gave the best correlation in each case. For example, the Marrucci, Turner and Richardson & Zaki equations were found to be the most appropriate for three different frother types, respectively. In another application of the drift-flux equations, Yianatos and Finch (1988) utilized the following correlation found by Dobby and Finch (1986) between gas rate (V_g) and bubble size (D_b) to calculate air fraction:

$$D_b = C_g V_g^{\,n} \ , \qquad [15]$$

where C_g corresponds to the mean bubble diameter at a superficial gas velocity of 1 cm/sec and is a function of frother concentration and sparger relative dimension. The constant *n* varies between 0.2 and 0.3, for a range of V_g between 1 and 3 cm/sec.

Based on the drift-flux concepts introduced by Wallis (1966), Zhou and Egiebor (1993) presented a series of correlations useful for understanding the interrelationships between bubble rise velocity by buoyancy (or drift):

$$Ubd = \left(1-\varepsilon_g\right)Ugs, \qquad [16]$$

the average bubble rise velocity in a swarm:

$$\frac{Jg}{\varepsilon_g} = Jg \pm Jl + Ubd\,, \qquad [17]$$

and the drift flux:

$$Jgs = \varepsilon_g\left(1-\varepsilon_g\right)Ugs = Jg - \varepsilon_g\left(Jg \pm Jl\right) \qquad [18]$$

where all terms are as defined previously and *Ubd* is the bubble drift velocity.

Zhou et al. (1993) questioned the assumption generally made that bubbles behave as solid spheres and studied the effect of frother on bubble rise. They presented yet another technique to estimate average bubble size by taking into account the presence of frothers. The bubble drift velocity in a liquid with surfactant was established to be given by

$$Ubd = \frac{Ub\left(1-k_g\varepsilon_g\right)^2}{\left[1-\left(k_g\varepsilon_g\right)^{\frac{5}{3}}\right]} \qquad [19]$$

$$\text{with } Ub = \frac{A\left[\left(1+3.36CcRv^2\right)^{0.5}-1\right]^2}{\left(2CcRv\right)^2}, \qquad [20]$$

which includes a constant *Cc* related to frother type and concentration and another empirical parameter k_g. *Rv* is the average bubble radius and *A* is a constant given by

$$A = \frac{\left(\rho_l - \rho_g\right)g}{9\mu}. \qquad [21]$$

The bubble radius is then given by

$$Rv = \frac{Bc^{0.5}}{0.84 - CcBc} \quad \text{and} \quad Bc = \left[\frac{Jg\left(1-\varepsilon_g\right)}{\varepsilon_g} + Jl\right]\frac{1-\left(k_g\varepsilon_g\right)^{5/3}}{A\left(1-k_g\varepsilon_g\right)^2} \qquad [22]$$

Xu, Finch and Uribe-Salas (1991) had previously reported the application of a drift flux model to obtain theoretical estimates of the maximum air rates and bubble surface area rates in flotation columns. They considered three different phenomena: loss of bubbly flow, loss of interface and loss of positive bias flow. Two equations were employed in this analysis:

$$J_g = Ut\varepsilon_g\left(1-\varepsilon_g\right)^{m-1} - J_l\frac{\varepsilon_g}{1-\varepsilon_g} \qquad [23]$$

and $$J_l = Ut\left(1-\varepsilon_g\right)^{m} - J_g\frac{1-\varepsilon_g}{\varepsilon_g} \qquad [24]$$

The gas rate at which $\frac{dJ_g}{d\varepsilon_g} = 0$ was defined as the maximum gas rate for bubbly flow, or the flooding point. The limiting value for loss of interface to occur was taken as the gas rate at which the air fractions in the pulp and froth zones become equal. On the other hand, the air rate at which the bias flow becomes zero was determined from the maximum air rate before onset of negative bias.

2.3.2 Froth Modeling

One of the major hurdles, if not the greatest, in the attainment of a complete column flotation model is the representation of the froth phase. Without the capability of predicting froth zone recovery and enrichment, any model of a column cell would be ineffective. Unfortunately, there are quite a few complex events taking place in a froth. A mathematical representation of all the aspects of froth expansion, stability, drainage and mobility seems a very overwhelming task, even in the two-phase system. When solids are present, a whole set of new factors has to be considered. They include the effects of the solids on bubble coalescence, the conditions leading to solid detachment, and the probability of particle collection under the froth hydrodynamic conditions.

In a flotation column, a distinctive feature of the froth phase is the addition of wash water at the top. This is done with the purpose of washing down entrained material and providing enough water so that the loaded bubbles flow to the overflow launder. The cleaning action also occurs through selective detachment of particles, which may then return to the collection zone. This phenomenon, usually referred to as froth dropback, gives rise to internal recycling and upgrading (or selectivity). Froth stability is another important factor in the effective separation and recovery of the mineral species since bubble coalescence plays a significant role in the detachment of particles. The study of all of these elements has brought about some progress in understanding the role of the froth characteristics in flotation. Nevertheless, their incorporation into a mathematical model has proven to be a difficult task.

A lot of the work published on the froth zone of a flotation column deals with the hydrodynamics and structure of two-phase froths. The cleaning zone of the column is

usually viewed as consisting of two or three main sections. Some workers have represented it as an expanded bubble bed followed by a packed bubble bed and a conventional draining froth (Yianatos et al., 1986). Others see it as an expanded bed below a shallow conventional froth (Goodall and O'Connor, 1991b), as shown in Figure 2.1. Moreover, other investigators describe it as a countercurrent washing zone with a froth layer at the top, both of which are composed of dodecahedral bubbles (Dobby and Finch, 1986; Ross and van Deventer, 1988). These two zones are often referred to as the stabilized froth and the draining froth, respectively.

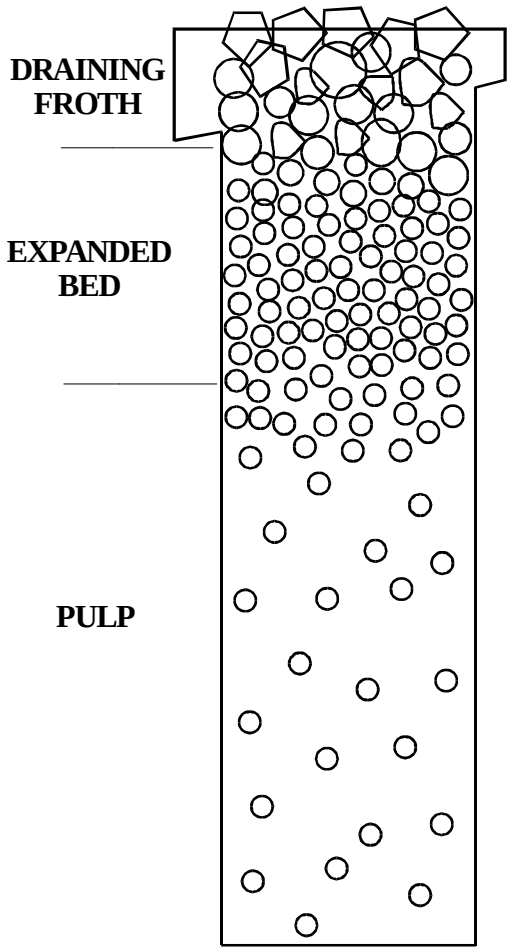

Figure 2.1: Column Hydrodynamic Zones

The foam models in the literature, which are based on a cellular structure with bubbles shaped as dodecahedral polyhedron, apply to conventional draining froths. In contrast, in the stabilized froth the bubbles are almost spherical due to the large liquid content (Yianatos et al., 1986). One approach is to regard this zone as an inverse fluidized bed (or expanded bubble bed) where the bubbles constitute the discrete phase

being held down by the downward liquid flow. As the bubbles rise through the expanded bed, they coalesce until they are large enough to overcome the slip force exerted by the liquid. The cellular foam forms when the bubbles get to be packed together.

An overview of some of the fundamental aspects of cellular foam models and fluidized beds might prove to be of interest. Such summary could add some insight into the methods followed by several investigators that have confronted the task of modeling column flotation froths.

• Cellular Foams

As bubbles grow in size in a packed bed, they can no longer sustain a spherical shape. Cellular froths are characterized by very high fractional gas volume and by bubbles whose shape can be approximated by pentagonal dodecahedra, resembling the structure depicted in Figure 2.2. The bubbles are packed so that, throughout the froth, the faces of three adjacent bubbles are arranged in a symmetrical fashion and so create liquid films which intersect at an angle close to 120°. The region where the films intersect constitutes a capillary channel, also known as a Plateau border in recognition of the studies performed by Plateau (Plateau, 1842-1868) on soap films.

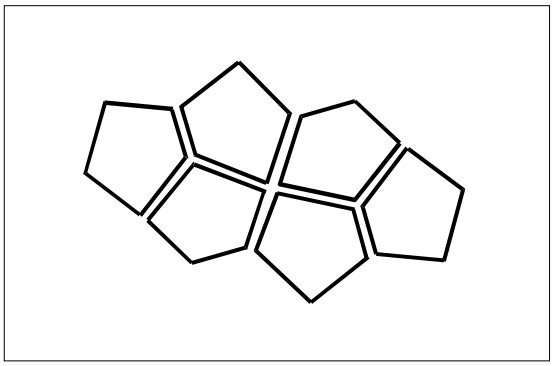

Figure 2.2: Cellular Foam Structure

Early investigations of the interstitial liquid flow in a foam were aimed at modeling foam drainage from a fundamental perspective, by writing a differential momentum balance within a Plateau border. The pressure difference Δp between the liquid in the Plateau border and the gas in the bubble is given by the Laplace and Young equation:

$$\Delta p = p_{out} - p_{in} = \frac{\gamma}{r} , \qquad [25]$$

where *r* is the radius of the Plateau border, represented in Figure 2.3, and γ is the surface tension. Drainage occurs from the film to the network of interconnected Plateau borders due to the pressure gradient caused by the curvature of the gas-liquid interface, and then down the borders due to gravity.

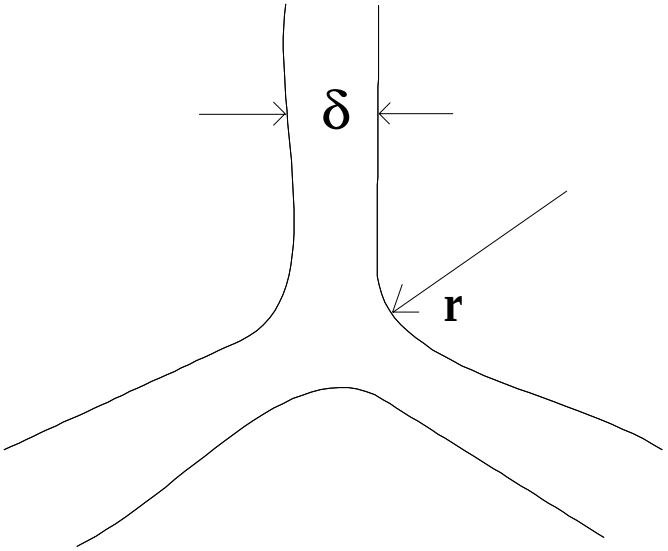

Figure 2.3: Plateau Border

A number of reports on the development of foam drainage models have in common such fundamental theory about capillary borders and draining films (Leonard and Lemlich, 1965; Haas and Johnson, 1967; Hartland and Barber, 1974; Barber and Hartland, 1975). However, the geometrical approximations used to represent the capillary channels vary. A cylindrical channel, a tapered channel, an equivalent diameter or nonrigid walls characterized by a surface viscosity are the alternative representations found in the literature. Since these models assume a steady state foam (amount of liquid entrained equal to the amount drained), they are not applicable to flotation unless they are modified to account for froth removal. Another assumption is that no coalescence takes place.

In the model of a stationary foam that utilizes the concept of an equivalent capillary diameter δ, the rate of thinning of the liquid channels is given by (Hartland and Barber, 1974)

$$\frac{\partial \delta}{\partial t} = - \frac{8 F \delta^{3}}{3 n^{2} \pi \mu R^{4}} \qquad [26]$$

and $F = \frac{\pi R^2 \sigma}{r}$ [27]

where F is the force acting on the film, δ is the film thickness at time t, n is the number of film surfaces rendered immobile by surfactants, μ is the film liquid viscosity, and σ is the surface tension. In addition, r is the radius of curvature of the Plateau border and R is the radius of a disk such that the disk area equals the area of a face of the dodecahedral bubble ($R = 0.3025d$).

Steiner, Hunkeler and Hartland (1977) utilized some of the concepts applied by Hartland and Barber. However, they assumed that the foam structure is carried upwards as a whole by the gas flow, and the liquid either flows down through the borders and films or is collected at the top. They also considered bubble coalescence to be a random process with a relationship between the probability of film rupture and the reciprocal of film thickness.

The amount of liquid being carried upwards that passes a unit horizontal plane per unit time is:

$$q_u = V_g \frac{1-\varepsilon_g}{\varepsilon_g} \quad [28]$$

which is also written as

$$q_u = q_d + q_t \quad [29]$$

where q_d is the downflow per unit area and q_t is the flow removed at the top. The total downflow is expressed as:

$$q_d = 8.845x10^{-3} \frac{\varepsilon^2 \rho g r^4}{\mu k_v d^2} \quad [30]$$

In Equations [27]-[29], V_g is the superficial gas velocity, r is the Plateau border radius, ρ is the liquid density, μ is the liquid viscosity, d is the length of the side of the dodecahedra, and g is the gravitational acceleration constant. The parameter k_v is a velocity coefficient, which is normally unknown. Expressions for the radius of the Plateau border, the film thickness, and change of film thickness with time and column height were provided by the authors. Simulation results for this model showed that, to obtain physically meaningful results, it is necessary to provide suitable estimates for the parameters.

• **Expanded Beds**

In a countercurrent flow at high liquid holdup, the relationship between the slip velocity of the particulate phase and the fluid is the same as that in an equivalent solid-liquid fluidized bed. Studies on countercurrent gas-liquid fluidized beds (Bridge, Lapidus and Elgin, 1964) have provided the basis for explaining the observed connections between gas rate, liquid rate and air holdup. These studies are also instrumental for predicting the flooding point and for understanding the influence of frothers on the slip velocity and the holdup.

In a packed bed, when gas initially enters at the bottom, the pressure drop across the bed increases with gas flowrate. However, at the moment when the flowrate produces a pressure gradient equal to the buoyant weight of the solids per unit volume, any increase in gas flow rate causes the bed to expand. The pressure drop then remains constant, and the void fraction increases. At even higher gas rates, bubbles are introduced and the bed becomes fluidized.

The treatment of fluidized beds in liquid-solids systems is analogous to that of sedimentation in the way the fluidizing velocity varies with voidage. This relationship was expressed by Richardson and Zaki (1954) with an empirical correlation that is mainly valid for high voidages:

$$\frac{U}{U_i} = \varepsilon_l^{\,n} \qquad [31]$$

where U_i is the particles free-falling velocity, U is the fluidizing velocity, and ε_l is the liquid voidage.

The major difference between the flow characteristics in fluidized beds and fixed beds is that the particles in a fluidized system are not fixed relative to one another. Therefore, for low voidage situations, similar equations could be applicable to both types of beds. A criterion normally followed to distinguish between packed beds and fluidized beds is that the maximum voidage in a packed bed is 0.26. Ergun (1952) developed the following equation for the pressure loss (ΔP) along a height L due to the flow of a fluid in columns packed with granular material (fixed bed):

$$\frac{\Delta P}{L} g = k_1 \frac{(1-\varepsilon)^2}{\varepsilon^3} \frac{\mu U_m}{D_p^2} + k_2 \frac{1-\varepsilon}{\varepsilon^3} \frac{G U_m}{D_p} \qquad [32]$$

where U_m is the fluid superficial velocity, G is the mass flowrate per unit area, Dp is the particle diameter, ε is the fluid volumetric fraction, g is the gravitational constant, μ is the fluid viscosity, and k_1 and k_2 are empirical constants. These pressure losses in packed beds were found to result from simultaneous kinetic and viscous energy losses with the viscous energy losses prevailing at low flow rates. Ergun's equation has become widely accepted

as a mechanistic representation of the flow through packed beds. Values of the two constants k_1 and k_2 need to be determined experimentally.

In the expanded bed the pressure gradient is given by

$$\frac{dP}{dL} = \left(\rho_s - \rho_f \right) g \left(1 - \varepsilon_l \right) \qquad [33]$$

which corresponds to the pressure drop where the bed begins to expand. Ergun's equation is still valid, so by eliminating the pressure gradient in both expressions, an equation relating the void fraction ε_l to the velocity can be derived (Ergun and Orning, 1949):

$$\varepsilon_l^3 - \frac{k_1 \mu}{D_p^2 \left(\rho_s - \rho_f\right) g} \left(1 - \varepsilon_l\right) U_m = \frac{k_2 \rho_f}{D_p \left(\rho_s - \rho_f\right) g} U_m^2 \qquad [34]$$

If the U^2_m is ignored (for low density, fine particles), an approximation for the previous equation is:

$$\frac{\varepsilon_l^3}{\left(1 - \varepsilon_l\right)} - \frac{\varepsilon_{l\,0}^3}{\left(1 - \varepsilon_{l\,0}\right)} = \frac{k_1 \mu}{D_p^2 \rho_s g} \left(U_m - U_{m0}\right) = c \frac{\Delta L}{L_0} \qquad [35]$$

which offers a way of estimating fluidized bed expansions from values at the incipience of expansion.

The fundamental studies on fluidized bed are pertinent to the area of column flotation modeling, particularly because of the structure of the stabilized froth region. In fluidized beds, the discrete phase normally consists of solid particles. However, an analogy between the bubbles and the particles can be drawn under the assumption that the bubbles in the froth behave as solid spheres. Another type of parallelism can be recognized in comparing the two systems. On one hand, in the stabilized froth the air bubbles rise by buoyancy against a liquid flow that opposes their direction of movement. In an expanded fluidized bed, the fluid opposes the settling of the particles, keeping them in suspension. Two expressions have been introduced (Equations [31] and [34]), which establish a connection between the air fraction and the relative velocity between the phases. Both have been applied on the representation of the flows in a column froth, as it will be described later on in this section. Two specific flows, liquid entrainment and drainage, are linked to the cleaning action in the stabilized froth.

Mathematical models that describe liquid entrainment and drainage for an air-water column operation were developed by Yianatos, Finch and Laplante (1986a) for each of the regions in the cleaning zone. The portion immediately above the interface is assumed to behave as an expanded bubble bed since the liquid holdup is usually more than 26%, which is the maximum liquid content supported in a packed bed. The draining froth, in turn, was represented as a packed bubble bed. A model of a dynamic cellular foam (Steiner, Hunkeler and Hartland, 1977) was slightly modified to represent the packed bed. The

amount of liquid entrained across a unit horizontal plane and the liquid flow down the films are given by Equations [28] and [30] respectively. The axial change of film thickness is calculated as

$$\frac{d\delta}{dh} = -\frac{29.13\delta^3 \varepsilon_g \sigma}{J_g \mu_l D_b^2 n_f^2 r \left[1 + \frac{0.0403(1-\varepsilon_g) D_b^4 \varepsilon_g \exp(-z^2/2)}{\delta^2 \varepsilon_g^2 s D_{bo}^3}\right]} \qquad [36]$$

with the radius of the Plateau border given by

$$r^4 = \frac{113.06 \mu_l D_b^2 k_v \left\{J_g(1-\varepsilon_g) - \varepsilon_g (J_C - J_W)\right\}}{\varepsilon_g^3 \rho_l g} \qquad [37]$$

The film thickness, taking into account the wash water, is then

$$\delta = \frac{0.304(1-\varepsilon_g) D_b}{\varepsilon_g} - 4.063\left[\frac{\mu_l k_v \left\{J_g(1-\varepsilon_g) - \varepsilon_g (J_C - J_W)\right\}}{\varepsilon_g^3 \rho_l g}\right]^{\frac{1}{2}} \qquad [38]$$

Coalescence was represented as a random process with a relationship between the probability of film rupture and the reciprocal of the film thickness. The probability of coalescence (or film rupture) is

$$z = \frac{\frac{1}{\delta} - \frac{1}{\delta_{ave}}}{s} \qquad [39]$$

The coefficient k_v was introduced previously; J_c, J_w and J_g are the superficial velocities of the product, wash water and gas streams, respectively. Other symbols include: n_f, which is a parameter related to the geometrical arrangement of the cellular foam; s, which is the variance of the film thickness distribution; σ, the surface tension; and ρ_l, the film liquid density.

To describe the expanded bubble bed, it was assumed that the channels through the bubble bed can be replaced by parallel pipes of variable cross-section characterized by a mean hydraulic radius. A modified friction factor for an expanded bed was obtained:

$$f = \frac{\left(1-\varepsilon_g\right) D_b \Delta P_f}{3\varepsilon_g U_l^2 \rho_l L_e} \qquad [40]$$

In Equation [40], ΔP_f is the pressure drop across the channel, L_e is the effective channel length, U_l is the liquid drainage velocity, ε_g is the fractional air content, ρ_l is the liquid density, and D_b is the bubble diameter.

The effective channel length was related to the bed height by a tortuosity model:

$$L_e = L\left\{1 - 0.5\ln(1-\varepsilon_g)\right\}, \qquad [41]$$

where L is the bed height.

For laminar flow, the following equations for the friction factor (f) and the Reynolds number (R_e) apply:

$$f = \frac{16}{R_e}\ ,\ R_e = \frac{deU_l\rho_l}{\mu_l}\ ,\ de = \frac{4D_b\left(1-\varepsilon_g\right)}{6\varepsilon_g} \qquad [42]$$

Combining equations, the superficial liquid drainage rate is

$$J_L = \frac{\left(1-\varepsilon_g\right)^3 {D_b}^2 \Delta P_f}{72{\varepsilon_g}^2 \mu_l L\left\{1-0.5\ln\left(1-\varepsilon_g\right)\right\}} = U_l\left(1-\varepsilon_g\right) \qquad [43]$$

The frictional pressure drop per unit length of the bed, ignoring the wall effects, is estimated as

$$\frac{\Delta P_f}{L} = \rho_l g\left[1-\varepsilon_g + \frac{J_W - J_C}{-J_W + J_C + J_g}\right] \qquad [44]$$

The drift flux equations have also been used to study the influence of the various flowrates on column operation and to characterize the flow behaviors in the froth and pulp zones (Pal and Masliyah, 1989; Langberg and Jameson, 1992). Pal and Masliyah utilized the drift flux model to prove the interconnection of the flow behaviors of the collection and froth zones. The expression that relates the net liquid flux in the froth to the gas rate and wash water rate is:

$$Jf = \frac{Qc - Qw}{A} = \left(1-\varepsilon_g\right)\frac{Jg}{\varepsilon_g} + Udg\left(1-\varepsilon_g\right), \qquad [45]$$

where the first term is the rate of liquid carried upwards and the second term represents the liquid drainage. In addition, Qc is the liquid flowrate leaving the column with the

concentrate, *Qw* is the wash water flowrate, and *A* is the column cross section. Here *Udg* equals $-Ugs$, where *Ugs* is the relative velocity between gas and liquid. In the collection zone,

$$Jf = -\frac{Qt}{A}. \qquad [46]$$

A considerable amount of experimental data is listed which was used to validate the drift flux model. The data proved that the ratio $\frac{Udg}{Ut}$ is just a function of air fraction and is independent of the flowrates. The experimental values were also employed to obtain a new drift flux correlation, better suited than the Richardson-Zaki correlation for air fraction values greater than 0.7:

$$\frac{Udg}{Ut} = 0.8\exp\left[-2.9\varepsilon_g{}^{2.1}\right] \qquad [47]$$

Langberg and Jameson also carried out an analysis of the hydrodynamic conditions for froth-pulp coexistence based on drift-flux theory. A dimensionless liquid flux, which is the same for both zones, was defined as:

$$\lambda_f = \frac{U_l}{U_g} = \frac{\varepsilon_l}{1-\varepsilon_l} - \varepsilon_l \frac{U_s}{U_g}\ , \qquad [48]$$

where U_l and U_g are the interstitial liquid and gas velocities, U_s is the bubble slip velocity, and ε_l is the volumetric liquid fraction.

The froth near the interface was treated as an expanded bubble bed with rigid spherical bubbles. Ergun's equation (Ergun, 1952) was used to model the base of the froth, close to the interface. The slip force per unit volume of the bed, consisting of the viscous and inertial drag forces, was equated to the expression of the slip force per unit volume for expanded gas-liquid beds:

$$F_s = \frac{K_1\left(1-\varepsilon_l\right)^2 \mu U_s}{\varepsilon_l D_b{}^2} + \frac{K_2\left(1-\varepsilon_l\right)\rho_l U_s{}^2}{D_b} = \left(1-\varepsilon_l\right)\varepsilon_l\left(\rho_l - \rho_g\right)g \qquad [49]$$

Combining the equations resulted in expressions for drag coefficient (C_D) and Reynolds number (R_e) for an expanded system:

$$C_D = \frac{K_1}{R_e} + K_2 = \frac{\varepsilon_l \Delta\rho g D_b}{\rho_l U_s{}^2}, \text{ and } R_e = \frac{\rho_l D_b U_s \varepsilon_l}{\mu\left(1-\varepsilon_l\right)}. \qquad [50]$$

Solving for Us yields:

$$U_s = \frac{K_1(1-\varepsilon_l)\mu}{2K_2\varepsilon_l \rho_l D_b}\left\{\left[1+\frac{4K_2\rho_l\Delta\rho g {D_b}^3{\varepsilon_l}^3}{{K_1}^2\mu^2(1-\varepsilon_l)^2}\right]^{\frac{1}{2}}-1\right\} \quad [51]$$

The range of applicability of this equation for monosized spherical bubbles was determined to be from ε_l = 0.26 to 0.7 (that is, air fraction between 0.3 and 0.74). An expression for flux based on the Ergun equation is then

$$\lambda_f = \frac{\varepsilon_l}{(1-\varepsilon_l)} - \frac{1}{BC}\left\{\left[(1-\varepsilon_l)^2 + B{\varepsilon_l}^3\right]^{\frac{1}{2}} + \varepsilon_l - 1\right\}, \quad [52]$$

where

$$B = \frac{4K_2\rho_l\Delta\rho g {D_b}^3}{{K_1}^2\mu^2} \quad [53]$$

and

$$C = \frac{K_1\mu U_g}{2\Delta\rho g {D_b}^2}. \quad [54]$$

Parameters *B* and *C* represent dimensionless bubble volume and dimensionless gas flux respectively.

Limiting conditions for the coexistence of both types of flow regimes and for countercurrent operation were obtained from the analysis. The countercurrent limit is given by:

$$\lambda_f = 0 \quad [55]$$

$$\text{and } \frac{\partial\lambda_f}{\partial\varepsilon_l} = 0 \quad [56]$$

The coexistence limit is given by Equation [56] and

$$\frac{\partial^2\lambda_f}{\partial{\varepsilon_l}^2} = 0 \quad [57]$$

If the Richardson-Zaki relationship is used, instead of the Ergun equation, and a similar analysis is performed, the limiting condition for countercurrent flow is found to be

$$\frac{U_g}{U_t} < \frac{(m-1)^{m-1}}{m^m}, \qquad [58]$$

where m is the exponent in Equation [9].

The limiting condition for regime coexistence is then

$$\frac{U_g}{U_t} < \frac{4m(m-1)^{m-1}}{(m+1)^{m+1}} \qquad [59]$$

The effects of air rate and bubble size on these limiting conditions were also investigated.

2.3.3 Bubble Coalescence

In bubbling systems, it is readily observable that small bubbles tend to fuse to form larger ones. In flotation systems, the presence of small bubbles is maintained through the addition of surfactants that reduce the surface tension at the air-water interface. Hence, the extent of bubble coalescence in the collection region of a flotation column is generally ignored. Coalescence in the froth regions, however, is much more apparent. More significant yet, it has a direct impact on the magnitude of the circulating load and, thus, the cleaning process. In addition, the froth carrying capacity, which limits the throughput, is a function of the available bubble surface area in the system. Consequently, in order for a column flotation model to be able to predict column performance adequately, bubble coalescence has to be taken into consideration.

Due to the different characteristics of the stabilized froth and the draining froth in a column, the phenomenon of coalescence is generally attributed to separate reasons. In the draining froth, coalescence appears to be a consequence of the drainage of the films between the closely packed polyhedral bubbles, while in the stabilized froth, collisions and oscillations are the probable causes. The bias water helps establish a distance between the bubbles to prevent deformation and film drainage. Gaudin (1957) proposed that, in a flotation froth, coalescence occurs only if the bubbles have surface space without loaded minerals. If that is the case, the probability of coalescence must be a function of the fractional bubble surface area that is not covered by mineral particles. A very similar conclusion was presented by Szatkowski (1995), who suggested that the more covered with hydrophobic particles the bubbles are, the less likely they are to coalesce. A conclusion of Gaudin's analysis was that the bubbles tend to keep a spherical shape when bubble loading is close to 100%, while they become large and polyhedral if poorly loaded. The current level of understanding about the causes and consequences of coalescence in flotation have not yet advanced to the extent where mathematical relationships quantifying this event are available. Some workers have attempted to follow the techniques described in cellular foam publications. However, those concepts are not applicable to the stabilized

froth region. For this reason, coalescence is normally not considered in any of the investigations of the stabilized froth although it has been observed.

Models of the coalescence mechanisms based on both collision and drainage have been proposed in other fields and reported. For instance, Argyriou et al.(1971) proposed a mechanism of bubble coalescence due to collisions in gas fluidized beds. The assumptions on which they based their study were: a) that the bubbles grow in size as they travel up the bed; b) that bubble frequency is reduced as bubble size increases; and c) that larger bubbles have higher velocities than smaller ones. The number of bubbles per unit height, the average bubble volume and the variance of the bubble volumes were determined by recording a video of the bubbles breaking at the top of the bed. A mathematical model was also developed by writing the conservation equation for bubble volume:

$$\frac{\partial f_{z,m,t}}{\partial t} + \frac{\partial \left(v f_{z,m,t} \right)}{\partial z} = h_{z,m,t} \qquad [60]$$

where z is the vertical position of the bubble, m its volume, f the number density, t the time, and h the net rate of introduction of bubbles by means other than flow (coalescence). The right-hand term can also be expressed as the difference between the rate of bubble formation (r_f) and the rate of disappearance (r_e):

$$h_{z,m,t} = r_f - r_e \qquad [61]$$

The rate of formation of bubbles of volume m, by the coalescence of bubbles of volume m' and m-m', was given by

$$r_f = \frac{B}{2S} \int f_{z,m',t} f_{z,m-m',t} \left[m'^{1/3} + (m - m')^{1/3} \right]^2 dm' \qquad [62]$$

and the rate of loss of bubbles of volume m, due to their coalescence with bubbles of volume m', was

$$r_e = \frac{B}{S} f_{z,m',t} \int f_{z,m',t} \left(m^{1/3} + m'^{1/3} \right)^2 dm' \qquad [63]$$

B is a function of the collision efficiency and the relative velocity of the colliding bubbles and S is the bed cross sectional area. The velocity as a function of volume was given the following form:

$$v = A m^{1/6} \qquad [64]$$

The model equations were solved for steady state after applying moment techniques to transform the integro-differential equations into ordinary differential equations and by assuming a gamma distribution. The set of ordinary differential equations yielded the profiles of the total number of bubbles (zeroth-moment), the mean bubble volume (first moment) and the variance of bubble volumes (second moment) along the bed height. These predicted profiles were compared to the experimental results from the video data. The model also indicated that the total number of bubbles per unit of bed height should decrease if the bed height increases, while the mean bubble volume increases. Bubble velocity was found to have a similar effect.

Another study of coalescence found in the literature was designed to measure the frequency of drop-drop coalescence in liquid extraction operations (Allak and Jeffreys, 1974). It was assumed that when the drops enter the bed, they remain spherical and arrange themselves in a compact way with a dispersed phase holdup around 0.76. This number corresponds to the maximum dispersed phase holdup value in fluidization. Above a holdup of 0.76, the drops take the shape of pentagonal dodecahedra, forming a dispersion band where the continuous phase drains from the films separating the drops. The film drainage induces coalescence. The thickness of this dispersion band is a function of initial drop size and dispersed-phase flowrate. The frequency of interdrop coalescence was found to depend on drop size, band thickness and the rate of drainage of the films. A correlation was found for the frequency of coalescence in terms of the capillary number:

$$\lambda_c = 1 - 0.559\left(\frac{\gamma}{\mu V_d}\right)^{0.054}\left(\frac{d}{H}\right)^{0.19} . \qquad [65]$$

In the equation above, λ_c represents the fraction of the total number of drops of mean diameter d that coalesce at a distance H from the entrance to the band. In the capillary number, γ is the surface tension, V_d is the drainage velocity, and μ is the liquid film viscosity. A model describing the drainage of the continuous phase film was written based on previous work on cellular froths (Leonard and Lemlick, 1965).

2.4 Three-Phase Models

2.4.1 Bubble-Particle Interaction in the Collection Zone

Since mineral flotation is mainly based on the concept of particle collection by bubbles, such phenomenon has received a lot of attention since the early days of flotation research. Most of the fundamental studies date back to the time before the development of flotation columns, with the interest in understanding the process of conventional flotation in cell banks. In this section, studies relating particle collection to cell turbulence are not considered since the objective is to look at the research relevant to column cells,

where quiescent conditions normally apply. Some of the examinations have emphasized the aspect of the hydrodynamics condition leading to bubble particle collision. Instead, other researchers have looked closely to the surface forces conducive to attachment. A few have reported on the circumstances that lead to particle detachment. Despite the ample literature on the subject, there is no consensus yet about the surface interactions at the microscopic level, particularly in relation to the hydrophobic force. Nonetheless, representations from first principles that encompass both the hydrodynamic and surface forces have been introduced recently. An important ally in the progress being made in that field is the advance in computation technology. Numerical solutions to fundamental fluid dynamics and force balance models are now achievable.

From early work (Schuhmann, 1942; Sutherland, 1948) particle collection has been regarded as a sequence of events that, together, determine its likelihood. First, a bubble and a particle approach each other until the liquid film between them thins. The film ultimately reaches a point called the critical film thickness, after which the film ruptures establishing a stable bubble-particle cluster that is not disrupted by particle inertia or turbulence. Three events, therefore, need to successfully take place. The first is the collision between the bubble and particle, which is determined by hydrodynamic conditions. The next event is the attachment of the particle to the bubble surface, which depends on hydrodynamics and surface forces. Finally, the third requirement is the stability of the bubble-particle aggregate, which means that the particle will stay attached to the bubble until it enters the froth. The probability of particle collection has been represented as a function of three parameters:

$$P = P_C P_A (1 - P_D), \qquad [66]$$

where P_C represents the probability of collision, P_A the probability of attachment and P_D the probability of detachment. Collection efficiency (or probability) has also been represented as the function of three physical quantities: the Stokes number, Reynolds number and the apparent particle settling velocity (Anfruns and Kitchener, 1976).

Gaudin (1957) also observed that after attachment the particles slide to the lowest part of the bubble surface. As a result, the probability of collection for other particles is reduced as the bubble becomes loaded. He suggested that when the fractional loading tries to increase above 50%, further particle collection is impaired. In their examination of flotation columns, Sastry and Fuerstenau (1970) indicated the need to include the change in available bubble surface area, due to increasing loading, in a process model. More recently, Sastry and Lofftus (1988) did so by incorporating the extent of bubble loading to the flotation rate term in a column flotation dynamic model. The same concept was applied in a column model for coarse particles, as Öteyaka and Soto (1995) introduced a new probability term, namely the probability of free bubble surface, in collection rate calculations. Dobby and Finch (1986) also showed the importance of considering bubble loading in scale-up calculations.

• **Bubble-Particle Collision**

The probability of collision has been defined as the fraction of particles in the path of a bubble that actually collide with it. In modeling the flow of particles past a single bubble, investigators have assumed quiescent conditions and that the flow pattern generated by the liquid around the bubble can be represented by a series of streamlines. The probability of collision is calculated based on a stream function by assuming that particle inertia is small and that particles follow the streamlines as they move past the bubble. In this way, the stream function provides the location of the particle with respect to the bubble. A limiting area is defined by the streamline which passes at a distance equal to the particle radius from the bubble equator. Only those particles inside that area have a chance of making contact with the bubble. That streamline is characterized by the radius R_O, measured at an infinite distance from the bubble. Therefore, from this definition, the probability of collision with a bubble of radius R_b is given by

$$P_C = \left(\frac{R_O}{R_b} \right)^2 \qquad [67]$$

neglecting the particle radius R_p.

The first mathematical expressions for the probability of collision were valid only for the condition of potential flow (very high Reynolds numbers) and Stokes flow (very small Reynolds numbers) (Gaudin ,1957):

$$P_C = 3\left(\frac{R_p}{R_b} \right) \text{(for potential flow)} \qquad [68]$$

$$P_C = \frac{3}{2}\left(\frac{R_p}{R_b} \right)^2 \text{(for Stokes flow)} \qquad [69]$$

Similar relationships were also developed by several other workers (Flint and Howarth, 1971; Reay and Ratcliff, 1973). They calculated the trajectories of particles in the path of a spherical bubble that is rising in an infinite volume of liquid and solved the equations of motion through different approaches. Flint and Howarth (op.cit) also considered the effect of the bubble swarm on the probability of collision as compared with the single bubble assumption. They estimated that the collision probabilities of particles with bubbles in a swarm can be several times as large as those calculated by solving the single-bubble model. However, no attempt was made to incorporate such effect into a mathematical relationship.

An expression applicable to a range of bubble Reynolds numbers was derived by Weber and Paddock (1983). Their expression for the probability of collision is:

$$P_C = \frac{3}{2}\left(\frac{D_p}{D_b}\right)^2\left[1+\frac{\left(3/16\right)Re}{1+0.249Re^{0.56}}\right] \qquad [70]$$

where *Re* is the bubble Reynolds number, D_p and D_b are the particle and bubble diameters. Jiang and Holtham (1986) also derived a general equation, which is

$$P_c = 6\left(\frac{0.3D_b}{0.58}\right)\left(\frac{D_p}{D_b}\right)^2 \qquad [71]$$

Later, Yoon and Luttrell (1989) derived a stream function for intermediate Reynolds numbers, since this range is more representative of the flotation process. Based on this stream function, a new expression for the probability of collision was given by:

$$P_C = \left(\frac{R_p}{R_b}\right)^2\left[\frac{3}{2}+\frac{4\cdot Re^{0.72}}{15}\right] \qquad [72]$$

This expression, along with the one developed by Weber and Paddock (1983), was then evaluated for a range of bubble diameters. The validation was carried out by way of experiments with highly hydrophobic material (probability of attachment is 100%). Both expressions agreed very well.

Clearly, the probability of collision increases with larger particles and smaller bubbles. Since the value of *Re* is a function of bubble size, the degree of dependence of P_C on *Rb* is not explicit.

Alford (1992) used a general form like the following:

$$P_C = \frac{D_p^2}{D_b^a} \qquad [73]$$

and determined that the values of *a* range between 0.2 and 0.6 for bubble sizes between 1 and 2 millimeters. Such conclusion was reached using an expression for collision probability developed by Dobby and Finch (1986b).

In a more recent study on the collision efficiency in countercurrent columns, Nguyen-Van and Kmet (1992) solved the Navier-Stokes equations for bubbles in a plug flow regime. Solids density, bubble slip velocity and particle settling velocity appeared to be major determinants of the collision efficiency, in addition to bubble size and particle size.

• Bubble-Particle Attachment

The probability of attachment is defined as the ratio between the number of particles that attach to the bubble and the number of particles in the bubble path.

Sutherland (1948) introduced the concepts of sliding time and induction time. Sliding time is the interval during which the particle slides over the bubble surface after collision. It is a function of both the liquid velocity around the bubble and the bubble size. The induction time is defined as the minimum time required for the thinning and drainage of the liquid film existing between the bubble and particle while the latter slides over the bubble. The probability of attachment has been linked to the magnitudes of these parameters since attachment cannot occur unless the induction time is shorter than the sliding time. The notion of a sliding particle has gained wide acceptance and it appears to be valid in a column, where turbulence is greatly reduced. For the analytical study of the probability of attachment a limiting region around the bubble was defined, which is characterized by a maximum angle θ_o. For an angle greater than such limit, the sliding time will be too short for attachment to take place. The probability of attachment is by definition:

$$P_A = \sin^2 \theta_O \qquad [74]$$

By applying the corresponding stream functions, the expressions for P_A for the potential, Stokes and intermediate flow conditions are (Yoon and Luttrell, 1989):

$$P_A = \sin^2\left[2 \cdot \arctan\left(\exp\left\{\frac{-3u_b t_i}{2R_b\left(R_b/R_p + 1\right)}\right\}\right)\right] \text{ (for Stokes flow);} \qquad [75]$$

$$P_A = \sin^2\left[2 \cdot \arctan\left(\exp\left\{\frac{-3u_b t_i}{2\left(R_b + R_p\right)}\right\}\right)\right] \quad \text{(for potential flow);} \qquad [76]$$

$$P_A = \sin^2\left[2 \cdot \arctan\left(\exp\left\{\frac{-\left(45 + 8Re^{0.72}\right)u_b t_i}{30R_b\left(R_b/R_p + 1\right)}\right\}\right)\right] \text{ (for intermediate flow)} \qquad [77]$$

The parameter u_b is the bubble rise velocity, while t_i represents the induction time. The studies on particle attachment have been numerous, since this event is intimately related to the general area of surface interactions and film thinning (Eigeles and Volova, 1960; Laskowski, 1974; Scheludko, 1976; Schulze, 1977, 1984 and 1989; Ye and Miller, 1988 and 1989; Li et al., 1990; Hewitt et al., 1995; Paulsen et al., 1996).

The probability of attachment was shown to increase with decreasing particle size and bubble size. However, if the bubble keeps getting smaller, it will reach a value at which P_A starts decreasing (Yoon and Luttrell, 1989). For very fine particles, there seems to be a consensus in the literature that P_A tends to unity independent of particle

hydrophobicity, which means that selectivity is lost (Yoon and Luttrell, 1989; Finch and Dobby, 1990; Li, FitzPatrick, Slattery, 1990).

• Detachment

In the analysis of flotation columns, the detachment of particles from the bubble surface before reaching the froth has not received much notice. Investigations on the maximum particle size that can be floated generally include the effect of turbulence in a flotation cell (Schulze, 1977; Holtham and Cheng, 1991; Cheng an Holtham, 1995). The other factors that determine the upper limit on particle size are the particle weight and the maximum buoyancy of the bubbles when loaded with particles. Crawford and Ralston (1988) studied the conditions for detachment in the absence of turbulence. They developed an expression for the maximum particle size from a balance of the capillary and gravitational forces, showing that the particle size upper limit depends on contact angle and particle density. This is in agreement with the work of Scheludko (1976), who gave an equation for the maximum attachment force of a particle as a function of contact angle and particle size.

• Fundamental Particle Collection Models

Several investigators have devoted themselves to obtaining a particle collection model derived from first principles. These models incorporate the roles played simultaneously by both hydrodynamic and surface forces on particle collection, rather than considering these forces independently, as the previous probability models do. A dynamic force balance was formulated by Schimmoller (1992), involving the gravitational, buoyancy, streamline-pressing, electrostatic, dispersion, structural and film-thinning-resistance forces. The resulting equation defines the force - attractive or repulsive - which determines the thickness of the film between bubble and particle. From the force balance equations in the radial and tangential directions, the changes in the particle position with time can be estimated.

In a more recent work, Yoon and Mao (1996) applied the extended DLVO theory to the development of a bubble-particle interaction model. Equation [66] is still applied in the model so that expressions for each of the probability terms have to be derived. To obtain the probability of collision, Equation [72] is employed. In the derivation of P_a, the energy barrier resulting from the combination of Van der Waals, electrostatic and hydrophobic forces were compared to the particle kinetic energy due to hydrodynamic forces. A condition for bubble-particle attachment was defined to be when the kinetic energy is greater than the energy barrier. The probability of attachment is finally represented using the following relationship:

$$P_a = \exp\left(-\frac{E_1}{E_k}\right), \qquad [78]$$

where E_1 is the energy barrier and E_k is the kinetic energy. The probability of detachment P_d is a function of the work of adhesion (W_a), the energy barrier (E_1) and a kinetic energy (E_k') that exceeds the sum of W_a and E_1.

$$P_d = \exp\left(-\frac{W_a + E_1}{E_k'}\right) \qquad [79]$$

Expressions for E_k and E_k' were obtained from an analysis of the streamline particle trajectory.

2.4.2 Mineralized Froth

In the first attempts to model the froth of a flotation cell, the froth was considered to be perfectly mixed (Arbiter and Harris, 1962; Harris and Rimmer, 1966; Bisshop and White, 1974). Lynch et al. (1974) later observed changes in solids concentration along the froth height in deep froths and assumed that when bubbles coalesce, the particles on their surface return to the pulp. Ball and Fuerstenau (1974) continued to use the perfect-mixer model, but incorporated a return rate from the froth to the pulp. A similar method was adopted in a recent publication (Hanumanth and Williams, 1992). In 1966, Cooper developed a plug-flow model for the froth phase (Cooper, 1966), and other investigators later followed suit (Mika and Fuerstenau, 1969; Sadler, 1973; Watson and Granger-Allen, 1974; Cutting and Devenish, 1975).

In the literature, the behavior of mineral particles in column flotation froths has been described in several instances using plug-flow models (Ross and van Deventer, 1988; Ross, 1991, Yianatos et al., 1988). These models generally follow the approach adopted by Moys (1978) to predict phenomena such as entrainment, drainage and detachment in conventional cells, in terms of first-order kinetic rates.

Moys (1978) assumed that each loaded bubble that reaches the base of the froth carries with it a surrounding slurry layer δ (Figure 2.4). The different velocities of the bubbles and the slurry cause the bubbles to pack together forming a cellular froth at the cell top. The air holdup increases with height as the liquid drains down the films separating the bubbles. In the model, particle detachment and particle entrainment are first-order processes characterized by rate constants k_d and k_e for each component. Detachment starts taking place above a particular distance from the froth base, which is where the available bubble surface area is reduced to zero due to coalescence.

The grade profile predicted by the equations was compared to experimental concentration gradients. In spite of the large number of adjustable parameters and the semi-empirical nature of the model, it was used as the basis for a study on the cleaning action and selectivity in column flotation froths.

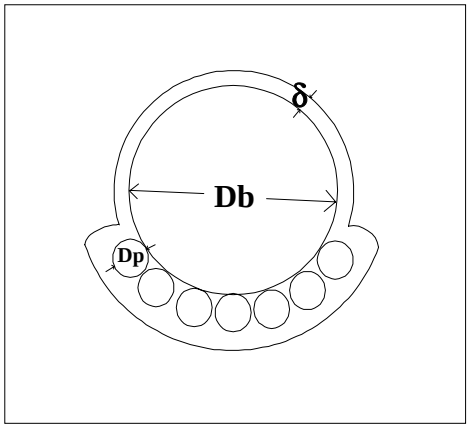

Figure 2.4: Mineralized bubble with slurry layer, as assumed by Moys (1978)

Yianatos et al.(1988) adopted the plug flow approach so that the change in the rate of attached particles along the froth as a consequence of detachment was expressed as:

$$\frac{dF_i(z)}{dz} = \frac{-k_i F_i(z)}{V(z)} \qquad [80]$$

where $F_i(z)$ is the mass rate of attached particles, belonging to species i, at height z; k_i is a detachment rate constant for species i; $V(z)$ is the bubble rise velocity at z, given by:

$$V(z) = \frac{V_g}{\varepsilon_g(z)} \qquad [81]$$

The solution to the differential equation above is given by:

$$F_i(z) = F_i(0)\exp\left[-k_i T(z)\right] \qquad [82]$$

where $F_i(0)$ is the rate at which the particles enter the froth and $T(z)$ is the residence time of the bubbles in the froth at height z:

$$T(z) = \frac{\int_0^z \varepsilon_g(z)dz}{V_g} \qquad [83]$$

The detachment rate constant k_i is assumed to be inversely proportional to the hydrophobicity of the mineral species. It is also assumed that no reattachment occurs in the froth. A washing rate constant is defined to calculate the rate $E_i(z)$ at which entrained particles are washed down the froth by the wash water. If C_i is the flowrate at the concentrate, the net rate of particles flowing down in the liquid is then:

$$R_i(z) = F_i(z) + E_i(z) - C_i \qquad [84]$$

The mineral mass fractions in the froth are obtained from the following equation

$$\frac{dM_i(z)}{dz} = \left[\frac{\{F_i(z) + E_i(z)\}\varepsilon_g(z)}{V_g} + \frac{R_i(z)\left[1-\varepsilon_g(z)\right]}{V_b} \right] \qquad [85]$$

and the grade is

$$G_i(z) = \frac{dM_i(z)}{\sum_j dM_j(z)}, \qquad [86]$$

while the percent solids along the froth height is given by the following expression

$$P_s(z) = \frac{100\sum_j dM_j(z)}{\left(1-\rho/\rho_s\right)\sum_j dM_j(z) + A_C\,\rho\left[1-\varepsilon_g(z)\right]dz} \qquad [87]$$

where A_c is the column cross sectional area, ρ is the water density, and ρ_s is the particle density. To solve these equations, the air holdup profile is assumed to have a parabolic shape. The air holdup at the concentrate level is estimated from the values of air rate and concentrate rate, and the air holdup at the froth base is given a typical value between 0.55 and 0.6. Experimental grade profiles and solids percentage profiles are fitted to the equations to determine the rate constants.

The detachment mechanisms considered in this model were a) drag caused by wash water and b) bubble coalescence. Although the authors recognize that selective reattachment is likely to occur in the froth, the model does not include a description of such mechanism. An increase in grade along the froth height was observed during the experimental work. Experimental results also indicated that a deep froth is needed in order to have froth selectivity (Yianatos et al.,1988).

A later report (Falutsu, 1994) indicated that dropback takes place throughout the froth in plant columns, but only at the interface in laboratory columns. The forces acting on a bubble-particle system were examined theoretically in an attempt to gain a better understanding of the mechanisms involved in froth cleaning. The drag forces exerted by

the bias water were estimated and their values compared to the forces holding the bubble and particle together. It was determined that drag forces are not a likely cause for particle detachment. A similar analysis was performed for the slippage of a particle along the bubble surface when the bubble decelerates and for the case of bubble oscillations. The conclusion reached from this study was that bubble deceleration when arriving at the interface and bubble oscillations tend to detach particles from the bubble surface. The process of reattachment was also theoretically discussed, but no conclusion was drawn due to the existence of several factors that either favor or hinder reattachment and the inability to quantify these factors. It was finally suggested that there exists a mixed layer just above the interface, and that although the froth eliminates entrainment, very little selective detachment takes place. The decreasing amount of solids with froth height that was observed was cited as an indication that no reattachment took place.

Another model based on Moys' mass transport approach was developed by Ross and van Deventer (1988) for column flotation froths. The froth was treated as two separate zones: a washing region and a froth layer. The same model was used for both zones. Detachment was attributed to bubble coalescence, while the contact and friction between loaded bubbles around the interface were neglected. Bubbles were assumed to be dodecahedral except in the first layer above the interface, where they were considered to be spherical. The mass flowrate of entrained material entering the froth was given by

$$m_{ei}(0) = \frac{X_i C_{\tau i} m_{eq}(0)}{C_{\tau q}} \qquad [88]$$

where X_i is a transfer factor for entrained species, $m_{eq}(0)$ is the mass flowrate of water entering the froth and $C_{\tau i}$ and $C_{\tau q}$ are concentrations of mineral and water in the pulp respectively. The mass flowrate of species that enter the cleaning region by flotation is:

$$m_{fi}(0) = m_{ti}(0) - m_{ei}(0). \qquad [89]$$

The thickness of the slurry layer around each bubble (δ) is estimated iteratively from the total flowrate of slurry, the amount of solids attached to each bubble and the bubble frequency. If there is not enough surface area to carry all the floating species, the least hydrophobic of the attached solids will be displaced at a height z_d above the interface. This particular position along the froth is a function of bubble size, frequency and particle size. The drainage of entrained particles is also assumed to be proportional to their concentration in the froth and the drainage rate constant is related to the distance between bubbles. A relationship between mean bubble size and height in the froth zones was developed which depends on the bubble size at the top and at the bottom of the zone along with the zone height. This expression was more applicable to the froth layer than to the washing zone where little coalescence occurs. Water concentration profiles and size fractions in the froth were measured and fitted to the model in order to estimate the necessary parameters.

In a more recent work, Moys (1984) used a two-dimensional streamline model to analyze the behavior of a well-drained froth. The solution of this model yielded streamlines for the bubbles in the froth. Froth stability, α, and residence time were defined in terms of the air leaving the concentrate, the air entering the froth, and a froth removal efficiency ξ. For simplification, Moys then divided the cross-sectional length of the pulp-froth interface into three stages with different stability and flow conditions. Using this three-stage model, he estimated the residence time distribution for perfectly floatable particles in the froth. Measurements of the RTD provided the model parameters α and ξ.

• Froth Stability

Froth stability has a very significant effect on the flotation process. When the froth is not stable enough, the bubbles rupture before they can be collected at the concentrate launder and the floatable particles are returned down the column. On the other hand, a froth that is too stable will also transport entrained gangue. The correct degree of stability is connected to the desired froth selectivity.

In a three-phase froth, stability is influenced by the particles and the surfactants present. Gaudin (1957) reported from his experience that the persistence of the froth is directly linked to the fraction of bubble surface covered by particles. Actually, the presence of particles seems to be necessary to achieve a stable froth (Szatkowski and Freyberger, 1985). Another observation made in that publication is that small bubbles are less likely to coalesce, especially when loaded. Frother reduces the bubble size and therefore promotes stability.

In addition, fine hydrophobic particles tend to destabilize the froth, especially at low concentrations, but coarse hydrophobic particles can prevent coalescence (Lovell, 1976). Hemmings (1981) showed that at low solids concentration the particles destabilized the froth, while at high concentrations the froth was stable. On the other hand, Dippenaar (1982b) observed a relationship between particle size and the solids concentration required for a constant degree of stability. He also reported (Dippenaar, 1982a) that film rupture occurs only when the lines defined by the three-phase contact with both bubbles migrate to the same point on the particle. This is the case for particles with a contact angle greater than 90°, or for irregular particle shapes even if the contact angle is less than 90°. Figure 2.5 illustrates the bridging of the film between two bubbles by an irregularly shaped particle as seen by Dippenaar (1982a).

From a study with quartz particles it was again shown that particle size and hydrophobicity have a profound effect on the characteristics of the froth and its stability (Johansson and Pugh, 1992). Both features are also inter-related so that small particles with low hydrophobicity appear to have very little influence on froth stability. On the other hand, for certain particle sizes there is an optimum degree of hydrophobicity, and the presence of these particles tends to strengthen the froth structure. Very hydrophobic particles, however, destabilize the froth by creating a bridge across the thin films.

Subrahmanyam and Forssberg (1988) summarized the information available at that time about froth stability, along with entrainment and drainage. The froth destabilization at fine sizes and/or low concentrations has been attributed to hydrophobicity, while the improved stability at higher concentrations is due to an apparent increase in particle size by agglomeration.

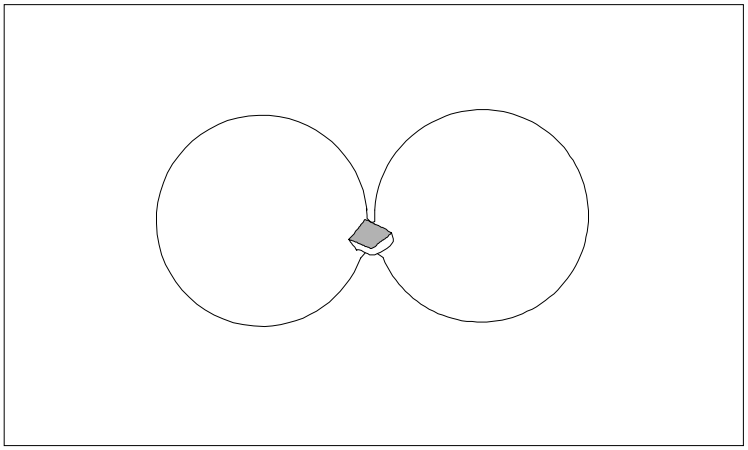

Figure 2.5: Film Rupture Caused by Particle (Dippenaar, 1982a)

2.4.3 Mixing

In countercurrent bubble columns, the swarm of bubbles rising against a downward flow of liquid causes a circulating flow pattern that results in axial mixing. The reason for such effect is that some of the liquid is entrained in the bubble wakes. In column flotation, quantifying the extent of mixing is necessary to predict recovery and grade. An increased axial mixing in a flotation column means that the process has deviated from plug flow behavior and, therefore, it affects the column performance.

Investigation of the axial mixing is generally carried out by analyzing the experimental residence time distributions (RTD) of the phases present in the column. RTD's are usually obtained by injecting a tracer at the top of column and recording the change in tracer concentration with time at the bottom. The residence time distribution data are used to fit either an axial dispersion model or a perfectly-mixed-tanks-in-series model. The axial dispersion model has one parameter: the vessel dispersion number, or its inverse, the Peclet number. The vessel dispersion number is defined as:

$$Nd = \frac{D}{uL} \qquad [90]$$

where D is called the axial dispersion coefficient, u is the interstitial liquid velocity and L is the column length. By definition, the higher the vessel dispersion number is, the greater the extent of mixing happens to be. The general form of the axial dispersion model is:

$$\frac{\partial C}{\partial t} = D\frac{\partial^2 C}{\partial x^2} - u\frac{\partial C}{\partial x}, \qquad [91]$$

where C is the concentration of material, x is the position in the reactor, and t is the time. In the tanks-in-series model, there is also one parameter; the number of perfectly mixed tanks, N. The higher the value of N, the closer the process is to plug flow behavior. There are two alternative ways of estimating the axial dispersion model parameter from the RTD data. One method is to use the following expression (Levenspiel, 1972) relating the variance of the distribution to the Peclet number (*Pe*) for a closed-end reactor:

$$\sigma = \frac{2}{Pe} - \frac{2}{Pe^2}\left(1 - \exp(-Pe)\right) \qquad [92]$$

Due to the amount of error in this technique, another approach has been recommended. The suggested method consists of generating RTD profiles for a series of values of the Peclet number and then choosing the optimum value based on a comparison with the experimental RTD data (Mavros, 1993). For the tanks-in-series model,

$$\sigma = \frac{1}{N}. \qquad [93]$$

The number of mixed zones is related to the dispersion coefficient through the equation:

$$D_l = \frac{N(N\cdot\theta)}{(N-1)!}\exp(-N\theta), \qquad [94]$$

where θ is a dimensionless time ($\theta = \frac{t}{\tau}$).

In chemical engineering there is extensive literature on mass transport in bubble column reactors, but most of these studies deal with flowrates that are much higher than those encountered in column flotation operations. Dobby and Finch (1985) first studied the mixing conditions in the collection zone of a flotation column and modeled it using an axial dispersion model. Their mixing representation assumed that the solid and liquid phases have approximately the same axial dispersion coefficient. They calculated the liquid dispersion parameter (D_l) from the measured RTD and found it almost linearly dependent on column diameter (D_C). The following correlation was proposed:

$$D_l = 0.063 D_C \left[\frac{\text{meters}}{\text{sec}^2} \right] \qquad [95]$$

They also found that the solids residence time is not affected by the bubble swarm at superficial air velocities lower than 3 cm/sec. Other workers have agreed with that observation (Yianatos, Finch, Laplante, 1986b). Since this original work, a number of investigators have performed studies on the residence time distributions of the liquid and solids in the collection zone of laboratory columns (Goodall and O'Connor, 1990; Goodall and O'Connor, 1992; Mills and O'Connor, 1990) and large industrial columns (Dobby and Finch, 1985; Yianatos and Bergh, 1990).

Goodall and O'Connor (1991b) proposed a model to describe the solids residence time distribution in a lab column cell. They used a tanks-in-series model for the pulp zone, a plug-flow-with-recycle model for the froth, and a mixed reactor with dead volume to describe the highly turbulent feed entry region. The utilization of the axial dispersion model for scale-up was discouraged because it was found to underestimate mixing in large columns. The reason is that the dispersion model is valid in cases that do not deviate significantly from plug flow, but industrial-scale columns operate in a well-mixed regime. Other investigators have arrived at a similar conclusion (Ityokumbul et al., 1995; Mavros et al., 1995; Mills and O'Connor, 1992). In another published review, Finch and Dobby advocate the plug-flow dispersion model. They claim that it is robust enough for plant columns since the dispersion number, though large, does not have to be accurately calculated (Finch and Dobby, 1990).

In another work, Goodall and O'Connor (1991a) employed the plug-flow-with-recycle model to investigate the interaction between the collection and froth zones. This type of model contains two parameters, which are the recycle ratio R and the plug flow residence time τ, as represented in Figure 2.6. The main objective of this work was to study the effects of air rate, pulp density and frother concentration on mixing (dispersion coefficient) in the pulp and froth regions and on column recovery and grade.

The influence of wash water and feed rate were described in a more recent publication (Goodall and O'Connor, 1992). In this case, both the tanks-in-series model and the dispersion model were used to describe the RTD in the pulp. It was observed that smaller bubbles in the pulp translated into greater plug flow behavior in the pulp and froth and higher recoveries and grade. Higher froth stability seemed to be related to a lower degree of mixing. Finally, shorter residence times in the pulp were observed to result in increased mixing.

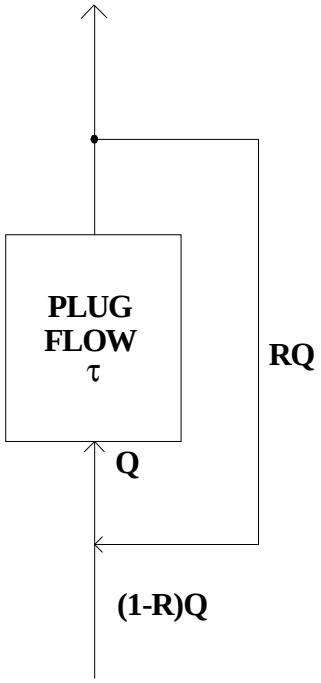

Figure 2.6: Plug-Flow-with-Recycle Model

A tanks-in-series model was the approach followed by Mavros et al.(1989) to characterize liquid mixing in an air-liquid flotation column. However, the authors stated that a one-parameter model cannot represent the liquid circulation patterns. The model had two parameters, the number of tanks *N* and a backflow coefficient λ which quantifies the liquid flowing backwards toward the top of the column, that is, the internal circulation. A large value of λ would indicate intense mixing. Block diagrams of a tanks-in-series model with and without backflow are shown in Figures 2.7 and 2.8 respectively. Mavros et al. (op cit.) also tested a new correlation, which related the model parameters to the Peclet number:

$$Pe = \frac{2N}{1+2\lambda} \qquad [96]$$

More recently (Mavros, 1993b), a procedure to estimate the backflow coefficient independently from *N* was developed, while λ was correlated to the superficial liquid velocity and the dispersion number. In another work, Laplante et al. (1988) suggested that the optimum fit of RTD's from lab columns to the simple tanks-in-series model is obtained with *N* between 10 and 30. For industrial columns, they recommend 2 tanks in addition to a larger perfectly mixed zone.

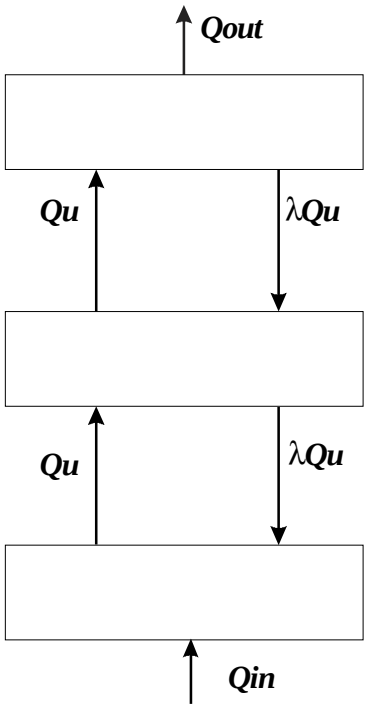

Figure 2.7: Tanks-in-Series Model with Backflow

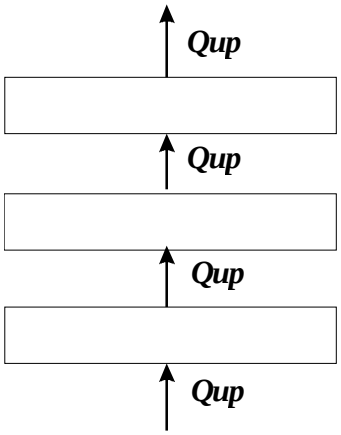

Figure 2.8: Unidirectional Tanks-in-Series Model

Several investigators have described experiments carried out at low flowrates in bubble column reactors to correlate the degree of mixing to the column diameter and gas rate (Baird and Rice, 1975; Todt et al, 1977; Joshi, 1980; Matsumoto et al., 1989). In later publications, a number of expressions for calculating the axial dispersion parameter in a flotation column have been proposed. In all cases, the equations relate the axial dispersion coefficient to the column geometry (D_C and H) and several operating parameters such as air velocity (V_G), liquid velocity (V_L) and air fraction.

a) $$D = 2.98 D_C^{1.31} V_G^{0.33} \exp(-0.025S), \qquad [97]$$

where S is the percentage of solids in the feed (Laplante et al., 1988)

b) $$D = 0.063 D_C \left(\frac{V_G}{1.6}\right)^{0.3} \qquad \text{(Dobby and Finch, 1986)} \qquad [98]$$

c) $$D = \left(9.3 D_C - 30.1\right) V_G^{0.603} \qquad \text{(Mavros, 1993)} \qquad [99]$$

d) $$N_D = \frac{1}{Pe} = 0.56 \left(\frac{D_C}{H_L}\frac{V_G}{V_L} Ugs\right)^{0.41} \qquad \text{(Xu and Finch, 1991)} \qquad [100]$$

e) $$Pe = B \left[\frac{H}{D}\frac{V_T}{V_G}\frac{1}{\left(1-\varepsilon_g\right)}\right]^m \qquad \text{(Mankosa et al., 1990)} \qquad [101]$$

In general, most of the authors seem to agree on a correlation of the form

$$D = K D_C^n V_G^m, \qquad [102]$$

which confirms that mixing is greater in industrial columns with large diameters than in lab columns, and that mixing is, to a lesser extent, a function of air rate. These types of correlations are very useful for scale-up. Mavros (1993a) attempted to verify some of these correlations using a set of experimental data. He concluded that correlations that do not take into account the air fraction within the column are unable to fit the data properly.

The assumption that solids axial mixing can be represented by the same parameter that characterizes liquid axial mixing is under contention, at least for large columns. Such hypothesis is based on previous studies with bubble columns that operate with larger bubble sizes and pulp velocities than flotation columns. Mills and O'Connor (1990) reported that solids could be more mixed than the liquid, and proposed that new

correlations be developed relating solids behavior and liquid mixing. These relationships would have to consider the impact of bubble size, feed percent solids, column diameter and gas flowrate. Of the expressions for the dispersion coefficient listed previously, only the one by Laplante et al. takes into account solids concentration.

The effect on mixing of the increase in air rate with height due to the decrease in hydrostatic pressure was also the subject of analysis by Laplante et el. (1988). Besides that subject, they examined the role played by the zone between the feed port and the interface. The collection zone was modeled as two zones of equal volume, with a higher value of the dispersion coefficient in the upper zone. Simulation results indicated that the use of only one dispersion coefficient was satisfactory and the authors did not consider it necessary to resort to compartment models. As for the part of the collection zone located above the feed port, it was found to act like a cleaning zone in laboratory columns. In large columns, on the other hand, it behaved as an extension of the recovery zone.

A different approach for modeling the flows in a flotation column is suggested by Deng, Mehta and Warren (1996). The authors consider that the axial dispersion model, as well as the tank-in-series model, does not provide enough detail about the process flows. They presented a two-dimensional, two-phase, fluid-dynamic model, which was solved numerically for several conditions.

As a way to reduce axial mixing, the use of baffles in the column has been proposed (Rice et al., 1974). However, in several instances, the presence of baffles enhanced mixing instead of reducing it (Mavros et al., 1995). Moys et al. (1993) studied the effect of several baffle geometries on the residence time distributions in a lab column. They reported that mixing is actually increased by the presence of baffles in the liquid phase because they divide the column into a series of parallel flow channels. The baffles seemed to reduce mixing if they extended above the interface. Utilization of multiple gas sparger was also found to increase mixing considerably, while the presence of a bed of packing material reduced it (Mavros et al., 1996).

2.4.4 Wash Water Effects

Mathematical relationships between wash water flowrate and column performance are rather scarce in the literature. From experiments carried out to determine the influence of wash water flowrate on recovery and grade, Weber et al. (1988) suggested that the optimum wash water rate for gangue rejection is a function of the column diameter (D_c) and is given by:

$$Q_w = 0.942 D_c^2 \qquad [103]$$

Later (Choung, Luttrell and Yoon, 1993), while examining the effects of varying the wash-water addition point, it was realized that this equation applied for a fixed wash-water addition point. The correlation was modified to predict the maximum wash water rate recommended at any position of the wash water inlet:

$$\max Q_w = 1.4137 D_c^2 \quad [104]$$

2.4.5 Column Flotation Kinetics

Kinetic models are commonly used in chemical engineering to describe numerous processes. The kinetic models of flotation are thus founded on the theory of chemical reactions. Since kinetics refer to the speed of a reaction or event, modeling of flotation based on kinetic behavior normally involves classifying the various particle types according to their specific flotation rate. These rates are a function of the particle composition and size.

Numerous investigators realized decades ago that the flotation process behaves roughly as a first-order process. Reviews of the literature on the initial applications of a first-order kinetic model to flotation are provided by Woodburn et al.(1965) and Fichera and Chudacek (1992). In its simplest form, this model is written as

$$\frac{dC}{dt} = k(C_0 - C) \quad [105]$$

which states that the rate of flotation is proportional to the mineral concentration *C* in the cell (Zuñiga, 1935). If the cell is perfectly mixed, the recovery of species *i* in a cell is then:

$$R_i = \frac{k_i \tau}{\left(1 + k_i \tau\right)}, \quad [106]$$

where *ki* is the flotation rate constant for the *i*-th species, and τ is the particle residence time.

For *n* cells in series, it is

$$R_i = 1 - \frac{1}{\left(1 + k_i \tau\right)^n}, \quad [107]$$

neglecting the froth volume. As for the non-floatable material, the recovery of the very fine particles is estimated to be directly proportional to water recovery:

$$R_i = e_i R_{water}, \quad [108]$$

where e_i is the degree of entrainment for a size class.

In a flotation column, the recovery is generally calculated using Levenspiel's equation, to account for the intermediate mixing.

$$R = 1 - \frac{4a \exp\left(\frac{1}{2N_d}\right)}{(1+a)^2 \exp\left(\frac{a}{2N_d}\right) - (1-a)^2 \exp\left(\frac{-a}{2N_d}\right)} \qquad [109]$$

$$a = \left(1 - 4k\tau N_d\right)^{\frac{1}{2}} \qquad [110]$$

Villeneuve, Guillaneau and Durance (1995) classified flotation models into three levels. The first level (Level 0) refers to models that define the recovery of each component for each bank and are made for material balance calculation; these models are referred to as performance models. The next two levels refer to predictive models that are usually based on the kinetic approach. These types of models are distributed first-order models that take into account the effect of particle size and particle floatability on the rate constants. The overall flotation rate is then a function of the sum of the rates for each size or floatability. In the Level-2 models, the rate constant distributions are first approximated by a discrete distribution of slow floating, fast floating and non-floating species. These models have two kinetic constants per mineral species. If a simplification is made by reducing the fraction of slow-floating material to zero, a Level-1 model is obtained. Another representation is to classify the material simply into floating and non-floating species, for each size class (King, 1973; Kelsall, 1961; Thorne et al., 1976). The size distribution can still be a continuous function (Huber-Panu, 1974).

Sutherland (1948) derived an expression to estimate the rate constant *k*:

$$k = 3\pi D_p D_b V N \operatorname{sech}^2\left(3V\tau/4R\right) \qquad [111]$$

where *k* is dependent on bubble size (D_b), particle size (D_p), relative velocity between bubbles and particles *V*, number of bubbles *N* and induction time τ. In terms of the overall probability of particle collection *P*, the recovery rate constant is given by:

$$k = \frac{3}{2} P\left(\frac{V_g}{D_b}\right) \qquad [112]$$

The expression for the flotation rate constant, according to the derivation performed by Yoon and Mao (1996) from a fundamental analysis of the collection process, is the following:

$$k = \frac{1}{4} S_b \left[\frac{3}{2} + \frac{4Re^{0.72}}{15}\right]\left(\frac{R_p}{R_b}\right)^2 \exp\left(-\frac{E_1}{E_k}\right)\left\{1 - \exp\left[-\frac{\gamma_{lv}\pi R_p^2 (1-\cos\theta)^2 + E_1}{E_k'}\right]\right\} \qquad [113]$$

The term S_b represents the superficial bubble surface area rate, R_p and R_b are the particle and bubble radii, E_k is the kinetic energy of the particle when approaching the bubble, while E_k' is the kinetic energy that detaches the particle from the bubble surface. Such parameters, along with Re (the bubble Reynolds number), relate the rate constant to the hydrodynamic conditions. In turn, θ stands for the contact angle, E_1 represents the energy barrier for bubble-particle attachment, and γ_{lv} is the surface free energy at the liquid-vapor interface. The latter three parameters belong to the realm of surface chemistry.

Modeling flotation as a kinetic reaction has become the general approach not only for describing the collection process, but also entrainment, drainage and detachment. Mika and Fuerstenau (1969) developed a mathematical model for conventional flotation, with a rate coefficient for each of nine different subprocesses. The rate mechanisms included backflow, entrainment, attachment in the pulp and in the froth, and detachment in both regions, as well. Four types of particles are assumed to exist: attached in the pulp, attached in the froth, free in the pulp and free in the froth.

In another flotation model (Hanumanth and Williams, 1992), the flotation cell was divided into three well-mixed zones, one pulp phase and two distinct froth phases. The processes of collection and entrainment were represented by two rate constants. One of them was an overall first-order rate of transfer from pulp to the first froth layer, and the other rate parameter accounted for mass transfer from the lower to the higher froth phase. The drainage of solids from the froth phases was also characterized by two first-order rate parameters. Unfortunately, the rate constants in these models are difficult to estimate from experimental data.

Szatkowski (1988) attempted to model flotation selectivity by incorporating the effect of bubble coalescence on flotation kinetics. One of the problems with this model is the series of simplifications that must be made. Another drawback is that the effects of the operating conditions on coalescence and collection efficiency were lumped into three empirical constants that need to be fitted to each particular system.

Column flotation is also generally modeled as a first order rate process. Recent work, for example, used a description based on the dispersed plug flow model to develop expressions of the rate parameters as functions of operating conditions (Napier-Munn and Lynch, 1992).

In spite of its general acceptance, the use of a first-order rate constant has been questioned. Arbiter (1951) suggested that particle collection in conventional flotation is a second-order process. Recently Ityokumbul (1992) pointed out for column flotation that, at high concentrations, recovery is indeed dependent on the initial concentration of floatable mineral due to the finite bubble surface area. In his design model, the rate of attachment is proportional to both the concentration of floatable material and the available bubble surface area. The rate of detachment depends on the fractional coverage of the bubbles. The net bubble loading is obtained by solving the equation:

$$\frac{d\Gamma}{dt} = k_a\left(\Gamma_m - \Gamma\right)C - k_d\Gamma \qquad [114]$$

where Γ is the fractional bubble loading, Γ_m the maximum loading possible, k_a is the rate of attachment, k_d the rate of detachment, and C the floatable mineral concentration.

The uncertainties in estimating the rate constants can be very significant. The sources of error are the deviations from first-order behavior, the plug-flow assumption, interaction between collection and cleaning zones, and feed characteristics among others (Del Villar et al., 1992).

2.4.6 Steady State Column Models

The information on bubble-particle interaction, column kinetic behavior and mixing is sometimes combined into an overall column flotation model. This type of model is normally applied to column design, scale-up, and performance prediction. The equations are normally valid for steady-state conditions and are not appropriate for real-time control.

Dobby and Finch (1986c) developed a column flotation model for scale-up. The model includes mixing and kinetic terms for both the collection zone and the cleaning zone. The dispersion coefficient for the solid and liquid phases is calculated with Equation [96], and the rate constant is obtained from the relationship

$$k = 1.5E_k\,\frac{V_g}{D_b} \qquad [115]$$

assuming that there are two floatable mineral species, fast floating and slow floating. The term E_k represents the collection efficiency (equivalent to the probability P in Equation [112]). Total recovery is a function of the recovery of the collection zone R_c, given by Levenspiel's equation, and the recovery in the froth R_k. The equation that relates the two recovery parameters is:

$$R_T = \frac{R_k R_c}{1 - R_k\left(1 - R_c\right)} \qquad [116]$$

The model keeps track of the degree of coverage of the bubbles to ensure that maximum loading is not exceeded.

Luttrell and Yoon (1991) developed a column simulator based on bubble-particle hydrodynamic interactions aimed at predicting column flotation performance with sulfide

minerals so that it could be utilized for scale-up, design and control. The column was divided into three zones: a pulp, a stabilized froth and a conventional froth.

The probability of particle collection by a bubble ($P = P_C P_A$) for each mineral component was first evaluated using Equation [72] to calculate Pc, while particle hydrophobicity, which is linked to P_A, was estimated from induction time measurements. The values obtained were employed in the calculation of a first-order rate constant ($k = 1.5P\frac{V_g}{D_b}$).

A volume balance of the flows into and out of the column resulted in

$$V_F + V_W = V_P + V_T , \qquad [117]$$

where V_F is the feed velocity, V_W is the wash water velocity, and V_T is the tailings velocity. The product velocity is

$$V_P = V_G \frac{\left(1-\varepsilon_g\right)}{\varepsilon_g} \qquad [118]$$

The bias water was estimated using the relationship

$$V_B = V_W - V_P , \qquad [119]$$

or $$V_B = V_T - V_F \qquad [120]$$

An optimum value of 0.25 cm/sec was recommended by the authors for the superficial bias rate based on experience. The Peclet number was used as a measure of axial mixing in this simulator. The value of this parameter was estimated using the empirical correlation obtained by Mankosa (1990), between the Peclet number, column geometry, liquid and gas flows and air fraction. The simulator was built for three components; fast, slow and non-floating. The carrying capacity, defined as the mass of particles that can be carried through the stabilized froth per unit column area, imposes a limit on recovery. Another limit is the froth overloading. In this simulator, when recovery exceeded either one of these restrictions, the excess material was assumed to return to the pulp (dropback). Using carrying capacity and froth overloading to set a circulating load was suggested as a way of improving grade.

Most of the column flotation models are applied to the flotation of fine particles. In a different kind of application, Ötekaya and Soto (1995) proposed a theoretical model for the flotation of coarse particles with negative bias rate. The froth phase is not considered because in such case it would be shallow. The flow of particles and bubbles was defined as plug flow (no mixing considered). The probability of particle collection was calculated as the product of four probability terms: probability of interception, which was expressed as

$$P_i = 1.209\sqrt[3]{\varepsilon_g^2}\,; \qquad [121]$$

the probability of collision, calculated with the equation by Jiang and Holtham (1986); the probability of aggregate stability, which in this case is the probability of detachment by inertial force,

$$P_s = \left(1 - \frac{D_p}{D_{p_{\max}}}\right)^3; \qquad [122]$$

and the probability that the bubbles are not fully loaded. To estimate the probability that bubbles are not fully loaded, it is assumed that particles slide to the bottom of the bubble, and when loading is less than 50%, the probability equals one. After the bubbles are more than half loaded, the probability starts decreasing until it reaches zero. Recovery is calculated by the following expression:

$$R = 1 - (1 - P)^n, \qquad [123]$$

where P is the overall probability described already and n is the number of elements in series in the collection zone. This model was found to be capable of predicting recovery as a function of the column length for a set of operating parameters, including bubble and particle sizes, gas rate and feed rate.

In an effort to use a flotation model for column design, Zhou, Xu and Finch (1995) applied a bubble-particle collision model for determining the minimum collection zone height for a flotation column. That height was found to be a function of bubble size, particle size, air fraction and bubble-bubble interactions.

2.4.7 Dynamic Models

The development of an accurate dynamic model is aimed at the incorporation of complex control systems strategies to flotation plants. The dynamic models of column flotation that are available can be classified into phenomenological (or mechanistic) models and empirical models. A mechanistic representation can help understand the processes that take place all at once because of its theoretical foundation. This type of models is being recommended for predicting column performance in applications such as model-based control and optimization (Herbst, Pate, Oblad, 1992). Nonetheless, empirical models can be very useful, particularly in industrial installations where the parameters of a more fundamental model can be very difficult to estimate. Some control systems can operate satisfactorily with empirical models, as long as the variations in the process are not excessive.

• **Phenomenological Models**

Phenomenological models can be fairly realistic representations, and they have received a lot of interest in the field of mineral processing. There is a general form for the model, but the parameters depend on each particular application. The parameter values can usually be correlated to operating variables, which is another advantage of this modeling approach. A type of phenomenological model that is especially appropriate for particulate processes such as flotation is the population balance model. The general form of the macroscopic population balance model is

$$\frac{1}{Vs}\frac{d[Vs\psi]}{dt}+\sum_{j=1}^{J}\frac{d[Vj\psi]}{d\zeta_j}+D-A=-\frac{1}{Vs}\sum_{k=1}^{K}Q_k\psi_k \qquad [124]$$

where ψ is the species concentration, V_s is the volume of the reactor, and ζ is a characteristic of the species represented by a distribution (such as size, mass, volume). The parameter V_j represents continuous changes in that distribution, D and A are the disappearance and appearance terms for reasons other than transport and Q_k stands for the flows into the reactor.

The first steps in the development of a dynamic model for the flotation process were carried out with flotation cells. A model developed specifically for control applications was the one described by Bascur and Herbst (1982). Their model has served as a foundation for more recent modeling efforts on column flotation. In this model, the flotation cell is divided into two volumes: the pulp volume and the froth volume. A liquid and an air phase are defined in each volume, and the particles are considered to be in either of these phases at any given time. The pulp was assumed to be well mixed, while the flow is treated as a lumped, spatially homogeneous volume. The attachment and detachment mechanisms were characterized by rate constants proportional to the number of particles in a given phase. The set of population-balance equations for free and attached particles, in the pulp and in the froth, was:

- for free particles in the pulp,

$$\frac{d\left(V_{LP}\psi_{i,j}^{LP}\right)}{dt}+k_{i,j}^{PAT}V_{LP}\psi_{i,j}^{LP}-k_{i,j}^{PDT}V_{BP}\psi_{i,j}^{BP}=Q_{Feed}\psi_{i,j}^{Feed}-Q_T\psi_{i,j}^{LP}+Q_Rk_{i,j}^{R}\psi_{i,j}^{LF}-Q_E\psi_{i,j}^{LP} \qquad [125]$$

- for attached particles in the pulp,

$$\frac{d\left(V_{BP}\psi_{i,j}^{BP}\right)}{dt}+k_{i,j}^{PDT}V_{BP}\psi_{i,j}^{BP}-k_{i,j}^{PAT}V_{LP}\psi_{i,j}^{LP}=-Q_A\psi_{i,j}^{BP}-Q_{AT}\psi_{i,j}^{BP} \qquad [126]$$

- for free particles in the froth,

$$\frac{d\left(V_{LF}\psi_{i,j}^{LF}\right)}{dt}+k_{i,j}^{FAT}V_{LF}\psi_{i,j}^{LF}-k_{i,j}^{FDT}V_{BF}\psi_{i,j}^{BF}=Q_E\psi_{i,j}^{LP}-Q_Rk_{i,j}^{R}\psi_{i,j}^{LF}-Q_C\psi_{i,j}^{LF} \qquad [127]$$

- for attached particles in the froth,

$$\frac{d\left(V_{BF}\psi_{i,j}^{BF}\right)}{dt} + k_{i,j}^{FDT}V_{BF}\psi_{i,j}^{BF} - k_{i,j}^{FAT}V_{LF}\psi_{i,j}^{LF} = Q_A\psi_{i,j}^{BP} - Q_{AC}\psi_{i,j}^{BF} \quad [128]$$

The symbols *V*, *k*, ψ, and *Q* represent the volumes, rate constants, number density of particles, and volumetric flows, in that order. The subscripts and superscripts in the previous equations are explained as follows:

i, size class*; j*, composition class*; L*, free; *B*, attached; *P*, pulp; *F*, froth; *E*, entrained; *R*, returned; *T*, tailings; *C*, concentrate; *A*, air; *F*, fed; *AT*, attachment; and *DT*, detachment.

The water volume balance equations are:

$$\frac{d\left(V_{LP}\right)}{dt} = Q_{Feed} - Q_T - Q_E + Q_R \quad [129]$$

$$\frac{d\left(V_{LF}\right)}{dt} = Q_E - Q_R - Q_C \quad [130]$$

In this model, the rate constants for attachment and detachment in the pulp were estimated from relationships applicable to impeller flotation machines. The rate of attachment in the froth was set equal to the number of bubbles rising through a froth height *Hf* per unit time, multiplied by the efficiency of collection by streamline interception. This collection efficiency was given by the ratio of the particle and bubble diameters (*Dp* and Db_f). Therefore,

$$k_{i,j}^{FAT} = k_j^{FAT}Q_A\left(\frac{Dp}{Db_f}\right)\left(\frac{Hf}{Db_f}\right) \quad [131]$$

In the consideration of detachment in the froth, the effects of two forces were taken into account: the shear force exerted by the fluid, and gravity. The entrainment flow Q_E was estimated from the assumption that bubbles entering the froth carry a sheath of water characterized by its thickness δ. The drainage flow Q_R is calculated using relationships provided by the studies on drainage through plateau borders in foams.

A column simulator (Lee, Pate, Oblad and Herbst, 1991) is based on the model described above. The simulator consists of a set of differential equations for a series of pulp and froth mixers. Once again, attachment and detachment are treated as first-order phenomena, and several size classes and compositions can be incorporated. Equations for particles in the *i*-th size class and *j*-th composition class, in the pulp, in the free and attached states respectively are:

$$\frac{d\left(V_{LP}C_{i,j}^{LP}\right)}{dt} = -k_{i,j}^{PAT}V_{LP}C_{i,j}^{LP} + k_{i,j}^{PDT}V_{BP}C_{i,j}^{BP} + Q_FC_{i,j}^{F} - Q_TC_{i,j}^{LP} + Q_RC_{i,j}^{LF} - Q_EC_{i,j}^{LP} \quad [132]$$

$$\frac{d\left(V_{BP}C_{i,j}^{BP}\right)}{dt} = k_{i,j}^{PAT}V_{LP}C_{i,j}^{LP} - k_{i,j}^{PDT}V_{BP}C_{i,j}^{BP} - Q_A C_{i,j}^{BP} - Q_{AT}C_{i,j}^{BP} \quad [133]$$

The analogous equations for any of the froth mixers are:

$$\frac{d\left(V_{LF}C_{i,j}^{LP}\right)}{dt} = -k_{i,j}^{FAT}V_{LF}C_{i,j}^{LF} + k_{i,j}^{FDT}V_{BF}C_{i,j}^{BF} - Q_C C_{i,j}^{LF} - Q_R C_{i,j}^{LF} + Q_E C_{i,j}^{LP} \quad [134]$$

$$\frac{d\left(V_{BF}C_{i,j}^{BF}\right)}{dt} = k_{i,j}^{FAT}V_{LF}C_{i,j}^{LF} - k_{i,j}^{FDT}V_{BF}C_{i,j}^{BF} + Q_A C_{i,j}^{BF} - Q_{AC}C_{i,j}^{BF} \quad [135]$$

In these equations, *C* is the particle concentration. The rest of the notation used above was already explained after Equations [122]-[125].

In a rather different way, the mechanistic dynamic model derived by Sastry and Lofftus (1988) incorporates an axially dispersed plug-flow model to represent the slurry and air phases. The model predicts the mass concentration of solids in the slurry and attached to air bubbles. Three main regions are defined in the column, which are a recovery region, an intermediate zone and a froth region. The rate of particle collection was assumed to be affected by the changes in free surface area on the bubbles. The detachment of particles was attributed to the flow of slurry down the column and was also characterized by a rate parameter. The equations obtained were too complex to be solved analytically, and a number of simplifications were made. One of the simplified versions of the dynamic model could be solved to predict the effects of changes in feed rate. The equations for any of the regions are:

$$\frac{\partial\left(h_w c_w\right)}{\partial t} = \frac{\partial}{\partial z}\left[D_w \frac{\partial c_w}{\partial z}\right] + \frac{\partial\left[\left(v_w + h_w v_s\right)c_w\right]}{\partial z} - k_a a_v f_{ss} c_w + k_d c_a \quad [136]$$

$$\frac{\partial\left(h_a c_a\right)}{\partial t} = \frac{\partial}{\partial z}\left[D_a \frac{\partial c_a}{\partial z}\right] + \frac{\partial\left(v_a c_a\right)}{\partial z} + k_a a_v f_{ss} c_w - k_d c_a \quad [137]$$

$$v_w = \frac{q_{wW} - q_{wP}}{A_C} \quad [138]$$

(in the intermediate and froth regions)

$$v_w = \frac{q_{wF} + q_{wW} - q_{wP}}{A_C} \quad [139]$$

(in the recovery region)

In these equations, the subscript *w* refers to the free state and *a* to the attached state. The *c*'s are concentrations; the *h*'s, lengths; the *q*'s, flows; the *v*'s, velocities; the *D*'s are

dispersion coefficients; k_a and k_d, attachment and detachment rates, respectively. The term $a_v f_{ss}$ accounts for the free space available on the bubbles.

Mankosa et al. (1990) developed a dynamic model based on a volume balance of the air phase in the collection zone that relates the air fraction to the average bubble size and the gas and liquid flowrates. If reduced to the steady-state form, it results in the drift-flux relationship. The model can be solved numerically and the authors intended to use it for bubble size estimations.

• Empirical Models

Development of an empirical input-output model entails a series of steps, which include the collection of appropriate data, selection of a model structure, estimation of model parameters and checking of the model. Discrete multivariate dynamic models relating the column operating variables have been derived and incorporated into model-based control strategies or into dynamic simulators. Bergh and Yianatos (1995) built a dynamic simulator for an air-water system. This simulator predicts the transient behavior of froth depth, air holdup and bias rate after a change in feed rate, wash water rate, opening of the tailings valve or opening of the air valve. Phenomenological models were avoided because of the difficulties in estimating model parameters from available data. The form of the discrete dynamic equations is

$$y_t = \frac{\omega\left(z^{-1}\right)z^{-b}}{\delta\left(z^{-1}\right)}u_t + \frac{\theta\left(z^{-1}\right)}{\phi\left(z^{-1}\right)\nabla^d}a_t \qquad [140]$$

where y_t is the output, u_t is the input and a_t is a white noise sequence with zero mean and constant variance. The symbols ω, δ, ϕ, and θ stand for different polynomials. Identification consisted of determining the polynomial orders and the values of b and d. The dynamic simulator was part of a data acquisition and control program.

From step or impulse responses, non-parametric models can also be built for control applications (Pu, Gupta, Al Taweel, 1991). The discrete convolution models obtained in this investigation were employed to develop a model predictive control system for a flotation column.

2.5 Summary

Modeling of the column flotation process requires combining the existing knowledge about a variety of phenomena that occur simultaneously during operation. A lot of the research on bubble-particle interaction was initiated decades ago, when people started to look into the scientific basis of froth flotation. The resulting models of the collection mechanism are also applicable to flotation columns, particularly when they

implicitly assume quiescent conditions. The effect of bubble loading on reducing the chances for the collection of more particles needs to be taken into consideration. This is especially true for conditions when the bubbles may become fully loaded. In addition, there is still a lot of uncertainty about the occurrence of particle collection in the froth, and how to represent it. The expressions for the pulp were derived from analysis of the interaction between just one bubble and one particle, but in the froth the bubbles are closely packed.

The representation of the flotation process as a kinetic reaction began when a number of workers observed a strong similarity between the recovery by flotation and a first-order chemical process. Since then, the recovery of particles in the pulp of a conventional cell, or in the column collection zone, is calculated as a function of a first-order rate constant and the mean residence time. However, mixing conditions in a flotation column are different from those in a conventional cell. Two main types of models have been used to represent mixing in columns, either a plug-flow dispersion model or a tanks-in-series model. Several reports favor the tanks-in-series technique, but a modification (backflow) has been suggested in order to make it more representative of the liquid circulation patterns observed in columns. Despite its drawbacks, the axial dispersion model is still employed.

The froth phase constitutes a great challenge for developers of mathematical models. A number of investigators have turned to previous developments in the areas of fluidization and foams in order to understand the structure of the stabilized froth and the draining froth. The progress made in other fields is very useful in the investigations of the occurrence of drainage and coalescence. However, the mathematical representations based on these fundamental studies have no practical application. Researchers are characterizing events such as drainage and detachment with first-order rate constants that have to be determined experimentally. The conditions for the estimation of these constants are often difficult to achieve, especially in industrial plants.

There are a few column flotation models reported in the literature that incorporate some of the elements discussed above. Most of these are steady-state models intended for column scale-up, design, steady-state simulation or optimization. The remaining models are dynamic models that either originate from conservation equations for all the phases, or empirical models derived for a specific application. A dynamic model is a crucial element of powerful control strategies that could help improve the operation of flotation columns. There are still a lot of complications to be addressed in the development of an adequate dynamic model. The complexity and the number of unknown parameters in the published models make it necessary to introduce a lot of simplifying assumptions. This measure reduces the predictive capabilities of such models.

2.6 Nomenclature

A_C: *Column Cross Sectional Area*
a_t: *White Noise Sequence*
C_g: *Constant Relating Gas Rate and Bubble Size*
Cc: *Constant Associated with Frother Type and Concentration*
$C_{i,j}$: *Mass Concentration of (i,j)-Particle Species*
C_i: *Mass Rate of Minerals Leaving with Concentrate*
D: *Dispersion Coefficient*
Db: *Bubble Diameter*
Dc: *Column Diameter*
Dp: *Particle Diameter*
Di: *i-th Species Diameter*
E_1: *Energy Barrier*
E_i: *Mass Rate of Entrained Minerals*
E_k: *Collection Efficiency/ Kinetic Energy for Attachment*
E_k': *Kinetic Energy for Detachment*
F_i: *Mass Rate of Attached Minerals Entering Froth*
$f_{z,m,t}$: *Number Density of Bubbles with Volume m, at Time t, and Height z*
g: *Gravitational Constant*
G: *Grade*
Jg: *Superficial Gas Velocity*
Jgs: *Drift Flux*
Jl: *Superficial Liquid Velocity*
k_1: *Empirical Constant in Ergun's Equation*
k_2: *Empirical Constant in Ergun's Equation*
k_g: *Empirical Constant in Equation [19]*
$k_{i,j}$: *Rate Constant for (i,j)-Particle Species*
L: *Height of Bubble Bed*
m: *Exponent in Richardson-Zaki Expression/ Bubble Volume*
m_e *Mass Flowrate of Entrained Material*
m_f *Mass Flowrate of Floated Material*
M: *Mass Fraction*
N: *Number of Tanks in Tanks-In-Series Model*
N_d: *Vessel Dispersion Number*
P: *Probability of Particle Collection*
P_A: *Probability of Bubble-Particle Attachment*
P_C: *Probability of Bubble-Particle Collision*
P_D: *Probability of Detachment*
Pe: *Peclet Number*
ΔP: *Pressure Difference Across Bubble Bed*
Q: *Volumetric Flowrate*
r: *Plateau Border Radius*
R: *Recovery*
Rb: *Bubble Radius*

Rp:	*Particle Radius*
Rv:	*Average Bubble Radius*
Re:	*Bubble Reynolds Number in a Single Bubble System*
Re_s:	*Bubble Reynolds Number in a Bubble Swarm*
R_i:	*Mass Rate of Minerals Draining from the Froth*
S_b:	*Superficial Bubble Surface Area Rate*
t_i:	*Induction Time*
u:	*Interstitial Liquid Velocity*
Ubd:	*Bubble Drift Velocity*
Ugs:	*Bubble Slip Velocity*
Ut:	*Bubble Terminal Velocity*
u_t:	*Model Input*
Vb:	*Bias Velocity*
Vf:	*Average Liquid Velocity*
Vg:	*Average Gas Velocity*
Vp:	*Concentrate Velocity*
Vt:	*Tailings Velocity*
Vw:	*Wash Water Velocity*
W_a:	*Work of Adhesion*
y_t:	*Model Output*
ε_f, ε_l:	*Liquid Holdup*
ε_g:	*Air Holdup*
μ_f, μ_l:	*Liquid Viscosity*
ρ_l,ρ_f:	*Liquid Density*
ρ_s:	*Solid Density*
ρ_i:	*Density of Species i*
ρ_{susp}:	*Suspension Density*
$\Delta\rho$:	*Density Difference between Continuous and Discrete Phases*
τ:	*Residence Time*
ζ:	*Discrete Phase Characteristic*
ψ:	*Number Concentration*
λ:	*Backflow Coefficient*
λc:	*Frequency of Drop Coalescence*
λf:	*Dimensionless Liquid Flux*
θ:	*Contact Angle*
θ_o:	*Maximum Angle for Attachment*
δ:	*Film Thickness*
γ:	*Surface Tension*
γ_{lv}:	*Surface Free Energy at Liquid-Vapor Interface*
Γ:	*Fractional Bubble Loading*